

AD _____
(Leave blank)

Award Number: **W81XWH-05-1-0593**

TITLE:

**Prostate Cancer Evaluation: Design, Synthesis and Evaluation of
Novel Enzyme-Activated Proton MRI Contrast Agents**

PRINCIPAL INVESTIGATOR: **Jian-Xin Yu, Ph.D.**

CONTRACTING ORGANIZATION:

**University of Texas Southwestern Medical Center at Dallas
Dallas, TX 75390-9058**

REPORT DATE:

October 2010

TYPE OF REPORT:

Final

PREPARED FOR: **U.S. Army Medical Research and Materiel Command
Fort Detrick, Maryland 21702-5012**

DISTRIBUTION STATEMENT: (Check one)

☒ Approved for public release; distribution unlimited

☐ Distribution limited to U.S. Government agencies only;
report contains proprietary information

The views, opinions and/or findings contained in this report are those of the author(s) and should not be construed as an official Department of the Army position, policy or decision unless so designated by other documentation.

REPORT DOCUMENTATION PAGE					Form Approved OMB No. 0704-0188	
<p>The public reporting burden for this collection of information is estimated to average 1 hour per response, including the time for reviewing instructions, searching existing data sources, gathering and maintaining the data needed, and completing and reviewing the collection of information. Send comments regarding this burden estimate or any other aspect of this collection of information, including suggestions for reducing the burden, to Department of Defense, Washington Headquarters Services, Directorate for Information Operations and Reports (0704-0188), 1215 Jefferson Davis Highway, Suite 1204, Arlington, VA 22202-4302. Respondents should be aware that notwithstanding any other provision of law, no person shall be subject to any penalty for failing to comply with a collection of information if it does not display a currently valid OMB control number.</p> <p>PLEASE DO NOT RETURN YOUR FORM TO THE ABOVE ADDRESS.</p>						
1. REPORT DATE (DD-MM-YYYY) 14-10-2010		2. REPORT TYPE Final		3. DATES COVERED (From - To) 15 SEP 05 - 14 SEP 2010		
4. TITLE AND SUBTITLE Prostate Cancer Evaluation: Design, Synthesis and Evaluation of Novel Enzyme-Activated Proton MRI Contrast Agents				5a. CONTRACT NUMBER W81XWH-05-1-0593		
				5b. GRANT NUMBER W81XWH-05-1-0593		
				5c. PROGRAM ELEMENT NUMBER		
6. AUTHOR(S) Jian-Xin Yu, Ph.D. Email: jian-xin.yu@utsouthwestern.edu				5d. PROJECT NUMBER		
				5e. TASK NUMBER		
				5f. WORK UNIT NUMBER		
7. PERFORMING ORGANIZATION NAME(S) AND ADDRESS(ES) University of Texas Southwestern Medical Center at Dallas 5323 Harry Hines Boulevard Dallas, TX 75390 - 9058 Jian-Xin.Yu@UTSouthwestern.edu				8. PERFORMING ORGANIZATION REPORT NUMBER		
9. SPONSORING/MONITORING AGENCY NAME(S) AND ADDRESS(ES) Department of the Army U.S. Army Medical Research and Materiel Command 504 Scott Street Fort Detrick, MD 21702-5012				10. SPONSOR/MONITOR'S ACRONYM(S)		
				11. SPONSOR/MONITOR'S REPORT NUMBER(S)		
12. DISTRIBUTION/AVAILABILITY STATEMENT Approved for public release; distribution unlimited						
13. SUPPLEMENTARY NOTES						
14. ABSTRACT The lacZ gene encoding E. coli beta-gal has already been recognized as the most commonly used reporter system in cancer gene therapy. Moreover, prostate-specific membrane antigen (PSMA) has been identified as an ideal antigenic target in prostate cancer. We propose to develop a novel class of Gd(III)-based MRI contrast agents for in vivo detection of beta-gal or PSMA activity. This new concept of the Gd(III)-based MRI contrast agents is composed of three moieties: (A) a signal enhancement group, such as Gd-DOTA or Gd-PCTA; (B) an Fe(III) chelating group; (C) beta-D-galactose or glutamate. Following cleavage by lacZ transgene or PSMA in prostate cancer cells, the released, activated aglycone Fe(III)-ligand will spontaneously trap endogenous Fe(III) at the site of enzyme activity forming a highly stable complex, to restrict motion of the Gd(III) chelates enhancing relaxivity and providing local contrast accumulation. We plan to synthesize 8 novel MRI contrast agents for imaging beta-gal or PSMA activity in prostate cancer cell culture, explore the feasibility of applying the most promising analogies to cells grown in vivo in mice and rats.						
15. SUBJECT TERMS Prostate Cancer Evaluation, Contrast Agent, Synthesis, MRI, Gene Expression, Gene Therapy, in vivo Cancer Imaging, lacZ Gene, beta-Galactosidase, PSMA, NAALADase						
16. SECURITY CLASSIFICATION OF:			17. LIMITATION OF ABSTRACT Unclassified Unlimited	18. NUMBER OF PAGES 31	19a. NAME OF RESPONSIBLE PERSON Jian-Xin Yu, Ph.D.	
a. REPORT Unclassified	b. ABSTRACT Unclassified	c. THIS PAGE Unclassified			19b. TELEPHONE NUMBER (Include area code) 214-648-2716	

Table of Contents

	<u>Page</u>
Introduction.....	4
Body.....	7
Key Research Accomplishments.....	17
Reportable Outcomes.....	17
Conclusion.....	17
References.....	19
Appendices.....	29

INTRODUCTION

BACKGROUND Prostate cancer is the most frequently diagnosed cancer and the second leading cause of cancer death in men in the United States, in 2009, approximately 192,000 men were diagnosed with prostate cancer with 27,000 succumbing to this disease,[1,2] currently, there is no cure for locally advanced or metastatic prostate cancer.

Gene therapy has emerged as a potentially promising strategy for treatment of prostate cancer.[3-15] The prostate is particularly amenable to gene therapy.[11-16] However, there are major issues in terms of assessing the delivery to target tissue, assessing the uniformity (versus heterogeneity) of biodistribution and determining whether the genes are expressed.[15-33] A viral construct is often readministered on successive occasions, but this should optimally be timed to coincide with loss of expression. Inevitably gene therapy has associated risks, and thus non-invasive *in vivo* determining the duration of gene expression in an individual tumor could greatly enhance the viability of the approach. Gene expression now is commonly monitored by *in situ* hybridization techniques or by introducing a marker gene to follow the regulation of a gene of interest. Since β -galactosidase (β -gal) activity is readily assessed by histology or in culture, in hosts as evolutionarily diverse as bacteria, yeast, and mammals, its introduction has become a standard means of assaying clonal insertion, transcriptional activation, protein expression, and protein interaction, *lacZ* gene encoding *E. coli* β -gal has already been recognized as the most commonly used reporter system.[34] A variety of *lacZ* gene reporters has been developed, such as colorimetric,[35-39] fluorescence,[40-53] chemiluminescence,[54-61] radiotracers for positron emission tomography (PET) or single-photon emission computed tomography (SPECT),[62-66] magnetic resonance imaging (MRI) probes,[67-69] and ¹⁹F-NMR approaches,[70-77] though most of them have only been utilized in *in vitro* detection, with a very few successful applications *in vivo* so far.[39,49,50,51,60,63-65,67,68,76,77] Therefore, the development of non-invasive *lacZ* gene reporter techniques based on appropriate molecules and imaging modalities is still a high desire.

The superb spatial resolution and the outstanding capacity of differentiating soft tissues have determined the widespread success of magnetic resonance imaging (MRI) in clinical diagnosis.[78] The contrast in an MR image is the result of a complex interplay of numerous factors, including the relative T_1 and T_2 relaxation times, proton density of the imaged tissues and instrumental parameters. It was shown that contrast agent causes a dramatic variation of the water proton relaxation rates, thus providing physiological information beyond the impressive anatomical resolution commonly obtained in the uncontrasted images. Contrast agents are widely used clinically to assess organ perfusion, disruption of the blood-brain barrier, occurrence of abnormalities in kidney clearance, and circulation issues.[78-82] The responsive MRI contrast agents holds great promise in the gene therapy arena.[83,84] The abilities of these contrast agents to relax water protons is triggered or enhanced greatly by recognition of a particular biomolecule opening up the possibility of developing MRI tests specific for biomarkers indicative of particular disease states and aiding in the early detection and diagnosis of tumors. Desreux *et al* [80,85] demonstrated that, by chelating Gd(phen)HDO3A with Fe(II) to form a highly stable tris-complex, as shown in **Figure 1**, the relaxivity increased 145% at 20MHz and 37°C from 5.1mM⁻¹s⁻¹ per Gd(III) in Gd(phen)HDO3A form to 12.2 mM⁻¹s⁻¹ in the tris-complex. Desreux *et al* [80,85] also synthesized another iron-sensitive MRI contrast agent with a tris-hydroxamate (**Figure 2**). After the tris-

hydroxamate groups formed a chelate with Fe(III) , free rotation at the Gd(III) centers was restricted, thereby increasing relaxivity by 57% from 5.4 to $8.5\text{mM}^{-1}\text{s}^{-1}$ at 20 MHz.

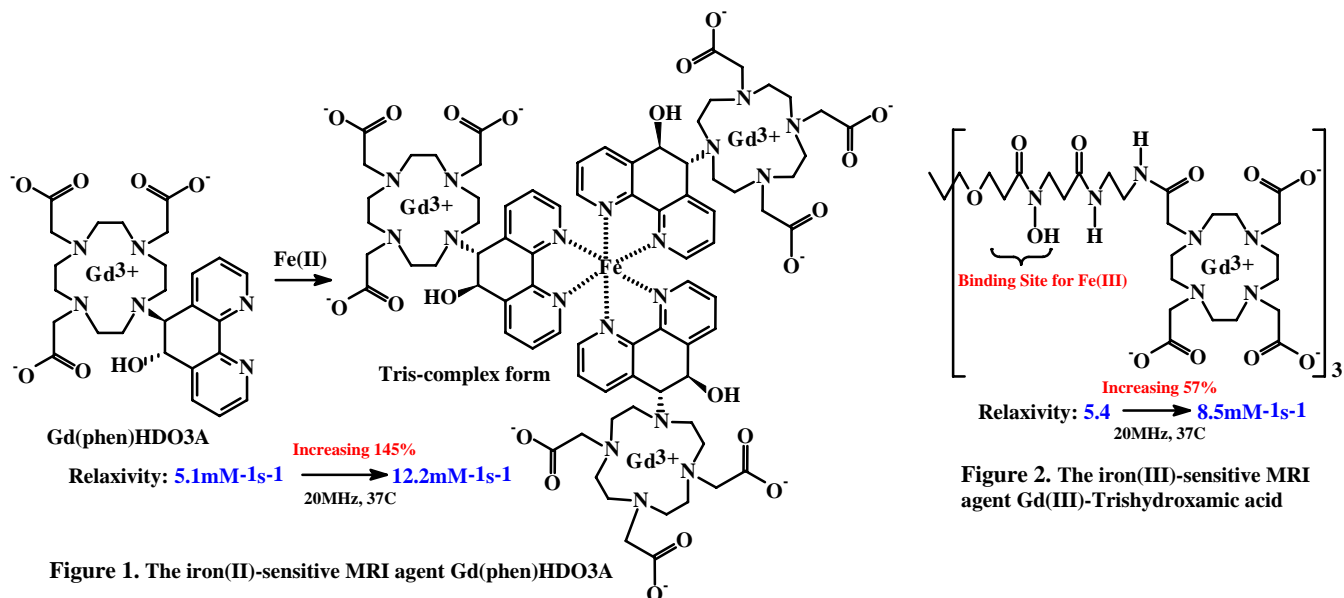


Figure 1. The iron(II)-sensitive MRI agent Gd(phen)HDO3A

Most recently, Merbach *et al* [86-88] observed the remarkably high T_1 relaxivity gain by the heterometallic, self-assembled metallostar formation with six efficiently relaxing Gd^{III} centers from $(\text{tpy-DTTA})\text{Gd}(\text{H}_2\text{O})$ with $7.3\text{mM}^{-1}\text{s}^{-1}$ to $\{\text{Fe}^{\text{II}}[\text{Gd}^{\text{III}}_2(\text{tpy-DTTA})_2(\text{H}_2\text{O})_4]_3\}^{4-}$ with $15.7\text{mM}^{-1}\text{s}^{-1}$ at 20MHz and 37°C (**Figures 3**), significantly, their detailed studies on structure and dynamics of the trinuclear complex $\{\text{Fe}^{\text{II}}[\text{Gd}^{\text{III}}_2(\text{tpy-DTTA})_2(\text{H}_2\text{O})_4]_3\}^{4-}$ indicate that the heterometallic self-assemblies attain high T_1 relaxivities by influencing three factors: water exchange, rotation, and electron relaxation.

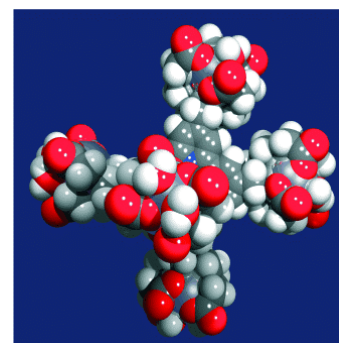


Figure 3. $\{\text{Fe}[\text{Gd}_2\text{L}_2(\text{H}_2\text{O})_4]_3\}^{4-}$

DESIGN Prompted by these findings, we proposed a novel class of enzyme responsive Gd^{3+} -based MRI contrast agent for high sensitivity and specificity for β -gal detection, based on the tumor biology and Fe-chelation therapeutic strategy. Cancer cells, as compared with their normal counterparts, exhibit increased uptake and utilization of more iron, as evidenced by an increase in transferrin receptors at the cancer cell surface, mediating a high level and rate of iron uptake.[89] More recently, an emerging class of Fe-chelator agents have shown effective antitumor activity *in vitro* and *in vivo*, which can overcome resistance to standard chemotherapy, due to their ability to affect multiple molecular targets including the enzyme responsible for the rate-limiting step of DNA synthesis, ribonucleotide reductase, molecules involved in cell cycle control (*e.g.* cyclin D1, $\text{p}21^{\text{CIP1/WAF1}}$) and the inhibition of metastasis (*i.e.* N-myc downstream regulated gene-1).[89-94] The FDA has approved five Fe-chelators for use in anticancer therapy so far, some others are in clinical trials for the treatment of various metastatic and solid cancers.[89,95-97] In our design, the *lacZ* responsive Gd^{3+} -based MRI contrast agent is comprised of three moieties: (A) a signal enhancement group, such as Gd-DOTA or Gd-PCTA ; (B) an Fe^{3+} chelating group; (C) β -D-galactose. Upon encountering with β -gal in tumor cells, the released, activated Fe^{3+} -ligand will spontaneously scavenge tumor abundant Fe^{3+} at the site of enzyme activity forming a highly

stable Fe-complex, to localize and accumulate the signal enhancement groups (*e.g.* Gd-DOTA or Gd-PCTA) in tumor, revealing regional β -gluc activity, and verifying the location and magnitude of tumor to evaluate the gene therapy. Also, the formation of the Fe-complex will restrict motion of the Gd^{3+} chelates, then enhancing additional relaxivity. **Figure 4** depicts the mechanism for detection of *lacZ* gene expression through Fe^{3+} -trapped MRI contrast agent formation.

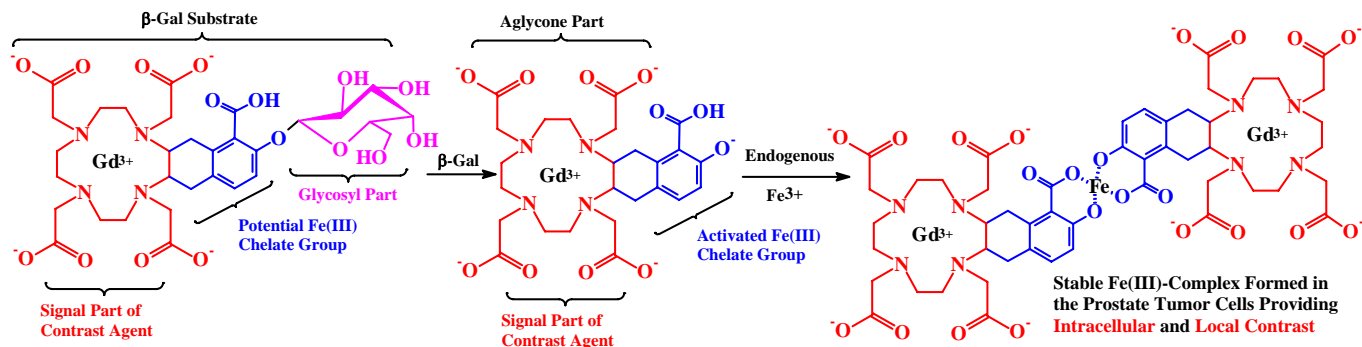


Figure 4. Detection of *lacZ* gene expression by β -gal activated *in situ* Fe^{3+} -trapped MRI contrast agent formation.

Prostate-specific membrane antigen (PSMA) is a type II transmembrane glycoprotein with enzymatic activities: N-acetylated α -linked L-amino dipeptidase (NAALADase) and γ -glutamyl carboxypeptidase (folate hydrolase).[97-99] Studies with the monoclonal antibodies have demonstrated that PSMA is the most well-established, highly restricted prostate cancer cell surface antigen, it is expressed at high density on the cell membrane of all prostate cancers.[100-102] The high prostate tissue specificity of PSMA has been identified as an ideal therapeutic and diagnostic target for prostate cancer, this potential was exemplified by the recent FDA approval of an ^{111}In -labeled PSMA monoclonal antibody (Prostascint[®]) for diagnostic imaging of prostate cancer.[103-110] Furthermore, phase I and II trials have begun using immunotherapy directed against PSMA.[106-108] By introducing γ -glutamate residue instead of D-galactose in the Figure 4, we intend to develop a novel class of PSMA responsive Gd(III)-based MRI approach specific for prostate cancers detection with high sensitivity (**Figure 5**).

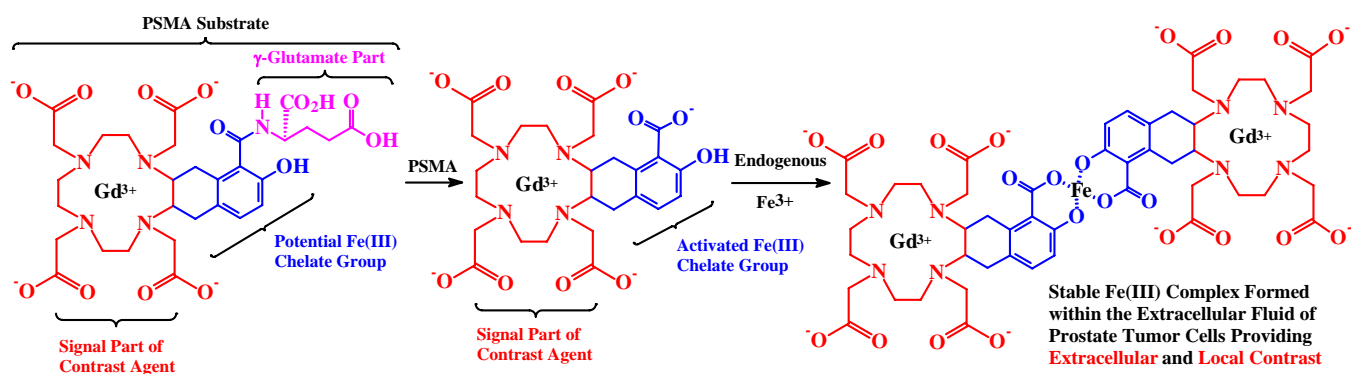


Figure 5. PSMA responsive Gd(III)-based MRI approach specific for prostate cancers detection.

Especially, PSMA has a large extracellular domain,[108] so the expression of PSMA tethered to the surface of the prostate cancer cells makes that the above novel peptide-based MRI contrast agents can be activated extracellularly around prostate cancers,[109] thus the need for a peptide-based MRI contrast agent to penetrate the prostate tumor cell membrane is no longer a prerequisite. The

permeability is always one of the greatest challenges in the development of *in vivo* MRI contrast agents.[111]

Accordingly, depending upon the enzyme sources either being the *lacZ* transgene or the PSMA from prostate tumors, this new platform could provide *in vivo lacZ* gene expression assay or *in vivo* prostate cancer imaging (in particular, through **extracellular** contrast agents), with combining the factors of reaching the high relaxivities. Furthermore, this new class of responsive MRI contrast agent is composed of three functional moieties, in which the signal enhancing and Fe^{3+} chelating parts are changeable allowing modification in a search for ideal Fe^{3+} -trapped MRI contrast agents. Importantly, the combination of three functional moieties is based on the clinically applied strategies on cancer therapy. These facts strongly suggest the potential of the proposal to future clinical application.

STATEMENT OF WORK

Specific Aim 1 Design and synthesize model “smart” MRI contrast agents to report β -gal or PSMA activities with the ability of trapping Fe^{3+} ion.

Task 1 Design and optimization of synthetic strategies for reporter molecules. **(Completed)**

Task 2 Structural characterizations of the synthesized molecules. **(Completed)**

Specific Aim 2 Test the properties of molecules in solution and *in vitro* with cultured prostate cancer cells.

Task 3 Evaluation the basic properties of the agents **in solution**. **(Completed)**

Task 4 Evaluation of the properties of the optimal molecules *in vitro* **with cultured prostate cancer cells**. **(Completed)**

Specific Aim 3 Scale up synthesis of the most promising MRI contrast agent(s) and apply to animal investigations.

Task 5 Scale up synthesis of the most promising ^1H MRI contrast agent(s). **(Completed)**

Task 6 Apply the most promising ^1H MRI contrast agent(s) to assess β -gal transfection efficiency, *lacZ* gene expression (spatial and temporal) in prostate tumors *in vivo*. **(Completed)**

Task 7 Test dosing protocols, timing, MR detection protocols **(Completed)**

Task 8 Prepare manuscripts and final report **(Completed)**

BODY

SEYNTHESIS Initially, we started the syntheses of the target molecules with the strategy of constructing the structures of Gd^{3+} and Fe^{3+} chelators simultaneously in the fused way as designed in the proposal, in order to maximize the restriction for the motion of the Gd^{3+} chelates, then obtaining the optimal relaxivity.

In the years 1 and 2, the syntheses according to the original plan met the challenges on (1) selective removal of benzyl ether (**in blue**) in the presence of benzyl ester (**in magenta**) by Pd/C hydrogenolysis; (2) selective removal of esters to accomplish the expected compound **D**, then to the target molecule **M₁** (see **Figure 6**). Because **M₃~M₆** are analogues of **M₁** and **M₂**, similarly, their syntheses had encountered the same situations. Although we put in much time and effort for solving these issues even partially in year 3, the failure made us modify the synthetic strategy by using tert-Butyl (instead of Ethyl) (see **Figure 7**), since they can be readily and selectively removed.

Prostate Cancer Evaluation: Design, Synthesis and Evaluation of Novel Enzyme-Activated ^1H MRI Contrast Agents

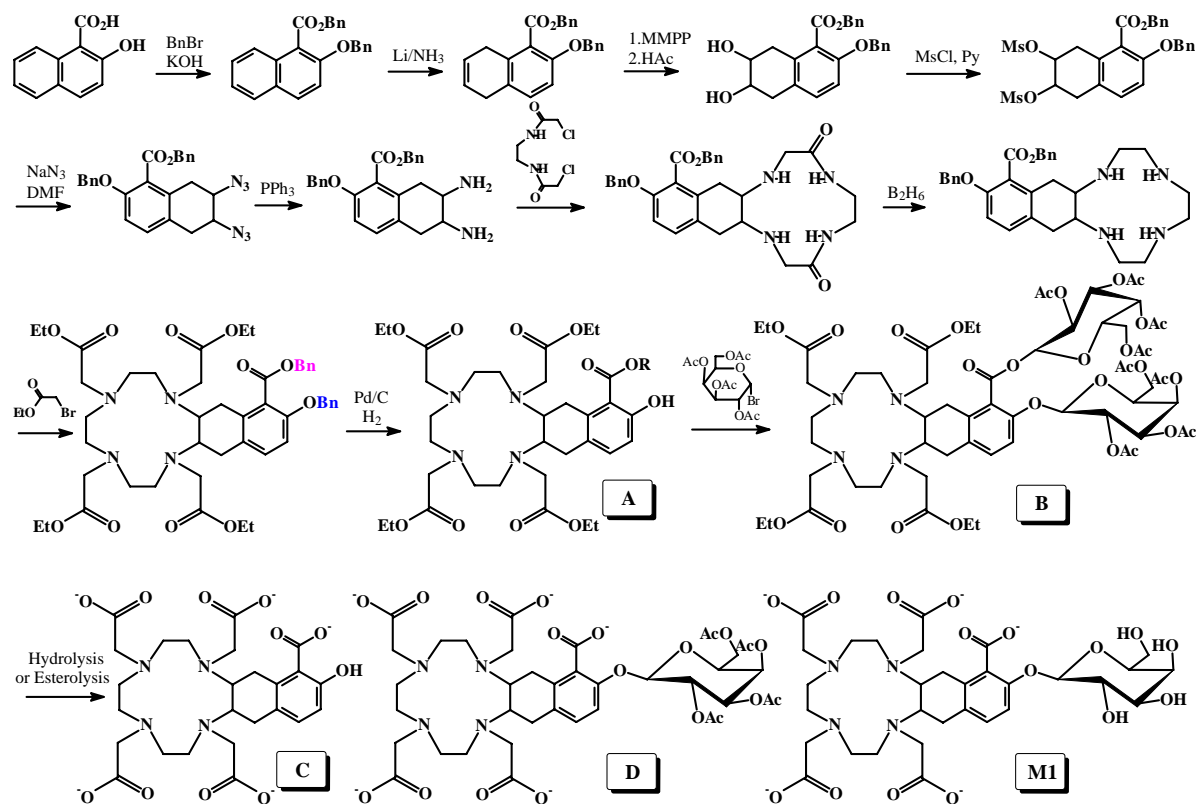


Figure 6. Initial Synthetic Strategies for $\text{M}_1\sim\text{M}_6$.

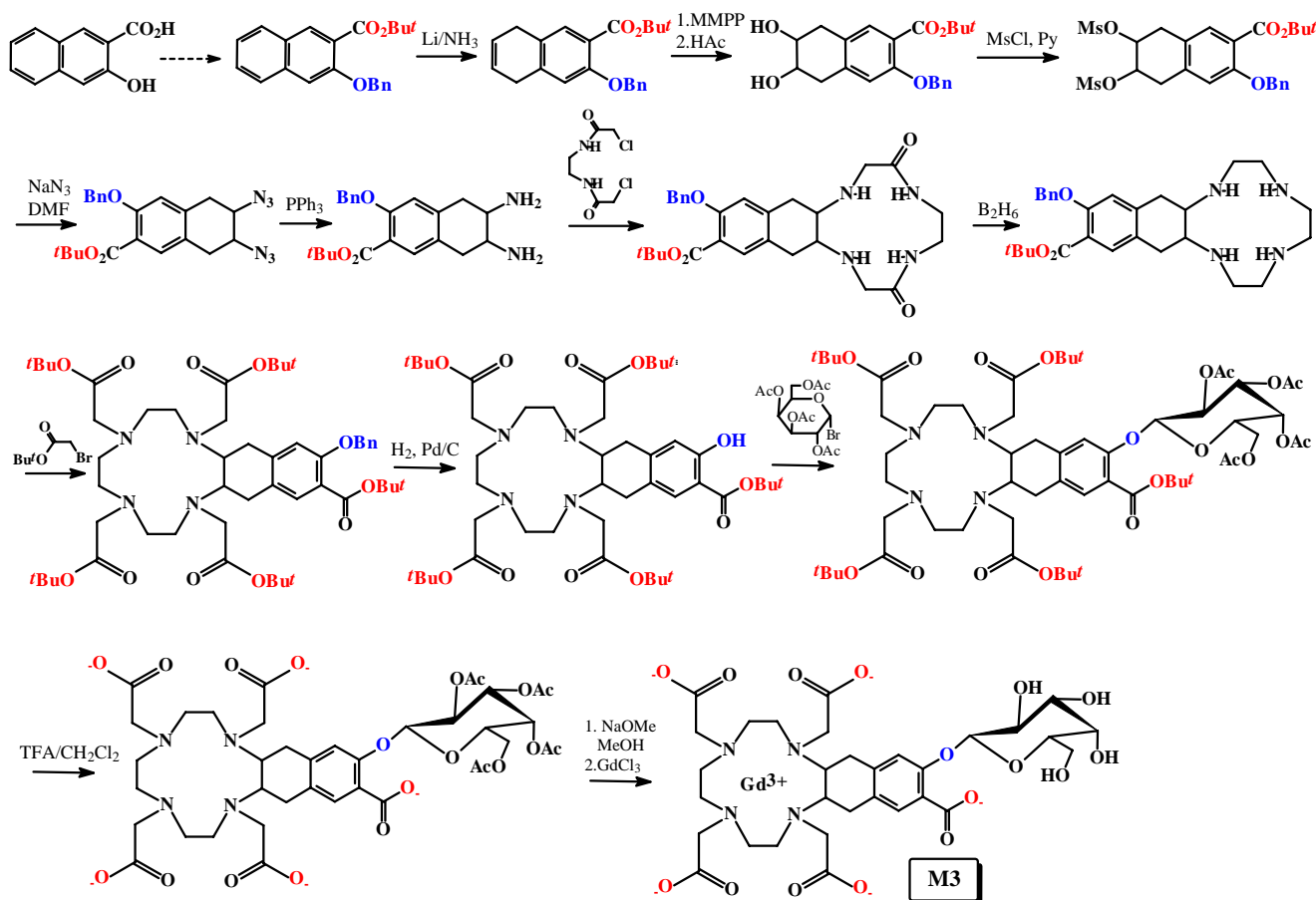
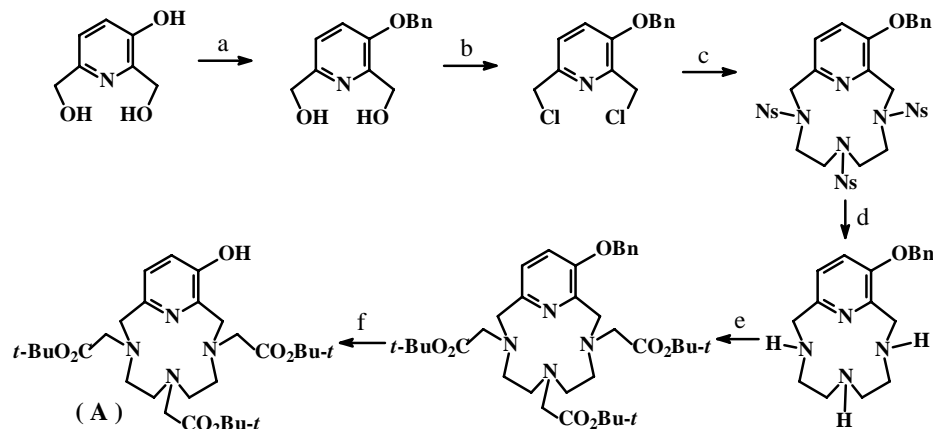
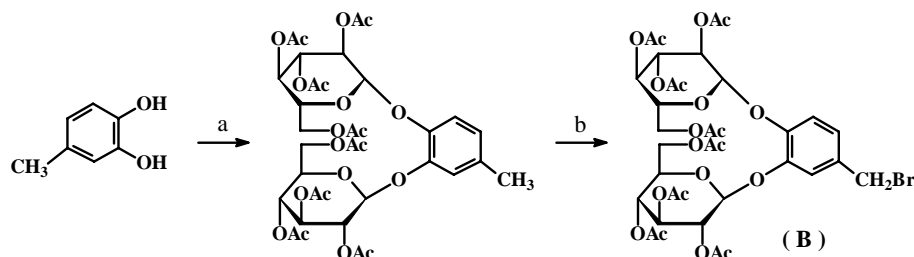


Figure 7. Modified Synthetic Strategies for $\text{M}_1\sim\text{M}_6$.

Following the modified synthetic strategy, we eventually achieved the designed target molecules $\text{M}_1\sim\text{M}_6$ and M_7 , M_8 (see Figure 8).



Reaction Conditions: (a) BnBr , K_2CO_3 , MeCN , 79%; (b) Bu_3P , CCl_4 , 80%; (c) $\text{NsNH}(\text{CH}_2)_2\text{N}(\text{Ns})(\text{CH}_2)_2\text{NH}_2$, K_2CO_3 , MeCN , 81%; (d) HSCH_2COOH , LiOH , DMF , 75%; (e) $\text{BrCH}_2\text{CO}_2\text{Bu-t}$, K_2CO_3 , 85%; (f) H_2 , Pd/C , 90%.



Reaction Conditions: (a) 2,3,4,6-tetra-*O*-acetyl- α -D-galactopyranosyl bromide, $\text{Hg}(\text{CN})_2$, 4 Å M.S., CH_2Cl_2 , 88%; (b) NBS , 78%;

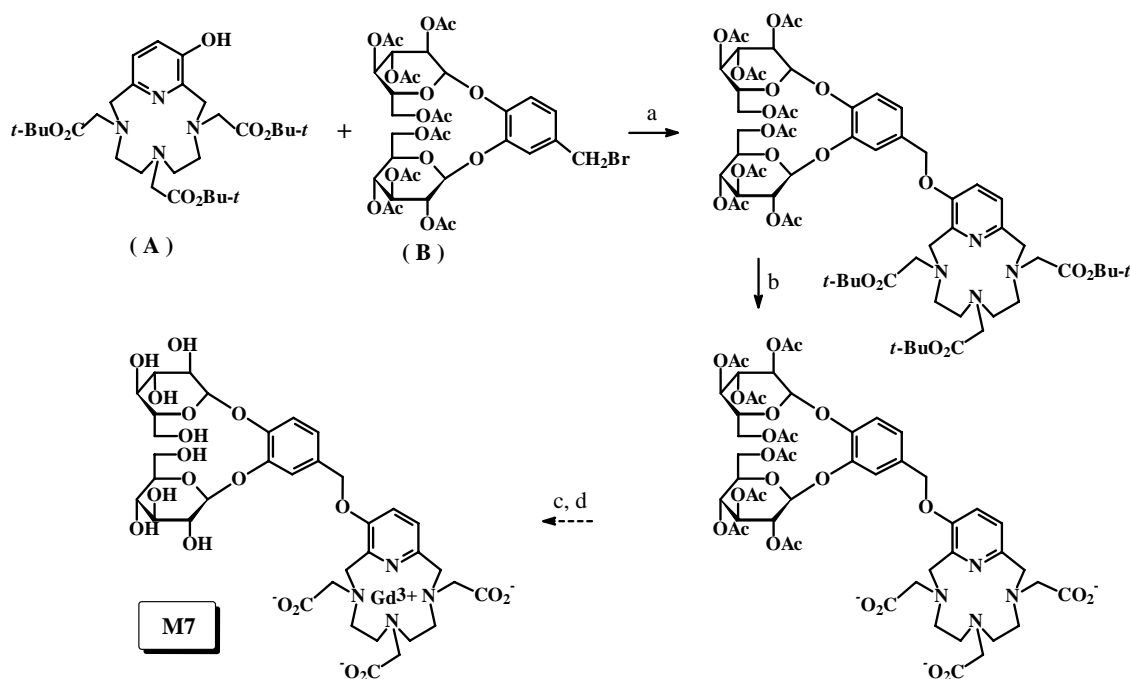


Figure 8. Reaction Conditions: (a) K_2CO_3 , MeCN , 75%; (b) $\text{CF}_3\text{CO}_2\text{H}$, CH_2Cl_2 , 81%; (c) GdCl_3 , Pyridine , 82%; (d) MeOH , MeONa , 89%.

The test of the target molecules $\text{M}_1\sim\text{M}_8$ using ^1H -MRI by comparing the contrast enhancement with that of the control in sodium phosphate buffer solution (PBS) (0.1 M, pH=7.4) in the presence of ferric ammonia citrate (FAC) with β -galactosidase E801A or PSMA (from lysed LNCaP cells in Tris buffer) indicated that: (1) the reporter molecules M_1 , M_3 , M_5 , M_7 can not be hydrolyzed by β -galactosidase E801A; (2) the reporter molecules M_2 , M_4 , M_6 , M_8 cannot be hydrolyzed by PSMA; so no MRI contrast changes before and after addition of β -galactosidase E801A or PSMA can be seen (**Figure 9** and **Table 1**).

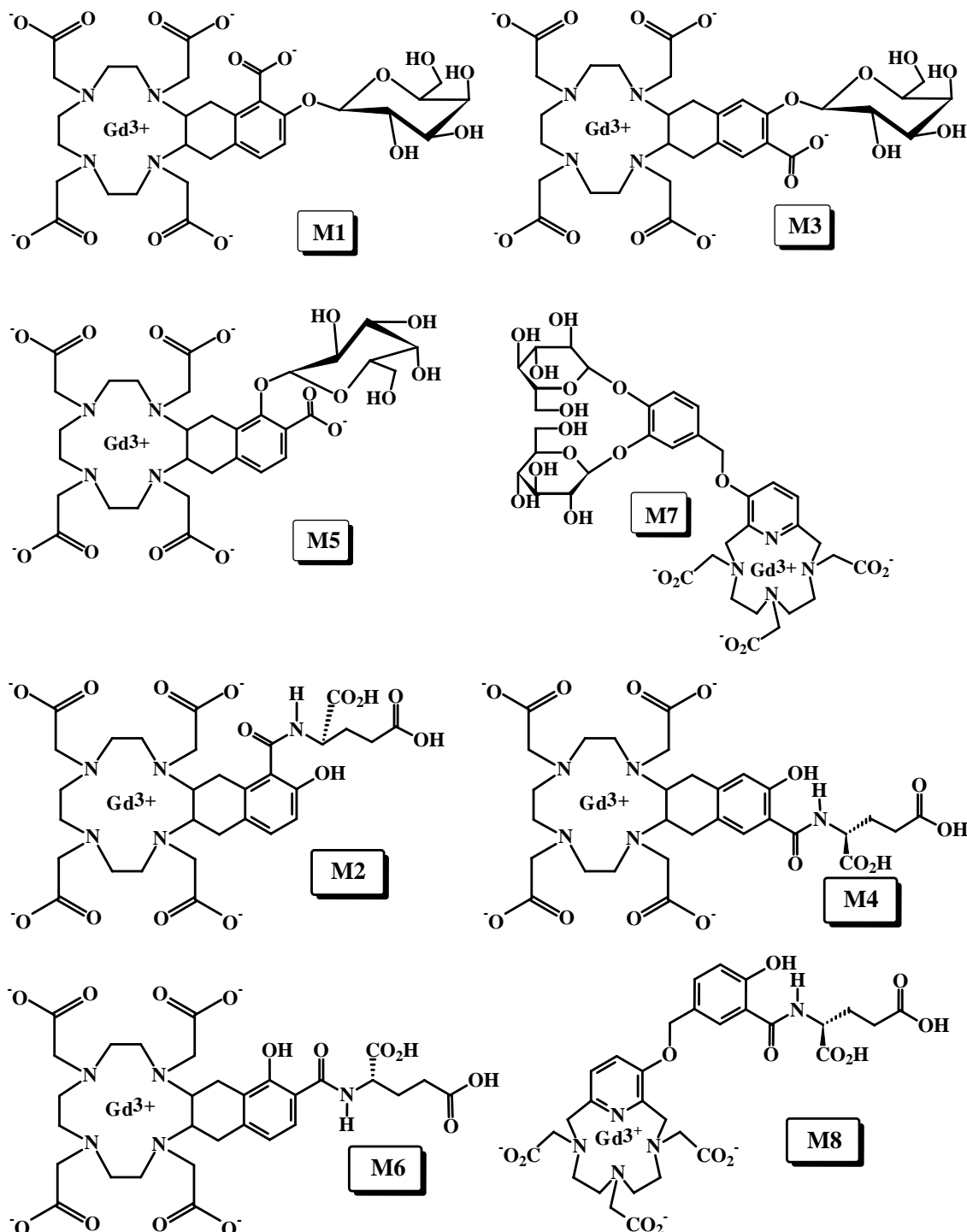
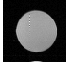
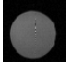


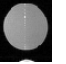
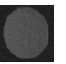
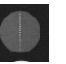

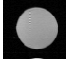
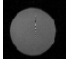


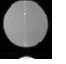
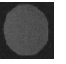
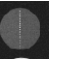



Figure 9

Table 1. ^1H -MRI contrast of the reporters $\text{M}_1\sim\text{M}_8$ in the presence of FAC. [Conditions: T_1 -weighted ^1H MRI, 200MHz, TR=300ms, TE=20ms, 1.5mm slice, 128×128, 50×50mm². (A) Control, M_1 , M_3 , M_5 , M_7 each (5μmol), FAC (2.5μmol), PBS (0.1M, pH=7.4, 1.5mL); M_2 , M_4 , M_6 , M_8 each (5μmol), FAC (2.5μmol), Tris buffer (50 mM, pH=7.4, 1.5mL); (B) Complex, $\text{M}_1\sim\text{M}_8$ each (5μmol), FAC (2.5μmol), E801A (10 units), PBS (0.1M, pH=7.4, 1.5mL)], or PSMA (from lysed LNCaP cells 5×10⁶), Tris buffer (50 mM, pH=7.4, 1.5mL).

Enzyme	β -galactosidase E801A				PSMA			
Molecule	M_1	M_3	M_5	M_7	M_2	M_4	M_6	M_8
T_1 -weighted ^1H MRI (Control)								
T_1 -weighted ^1H MRI (Enzyme)								

The molecular modeling shows that the fused structure of Gd^{3+} and Fe^{3+} chelator results in the molecular structures of $\text{M}_1\sim\text{M}_8$ very rigid (see **Figure 10** as an example of M_1 , M_2). Therefore, we deduced that these too rigid molecules would be hard to coordinate with PSMA or *lacZ* proteins and dock into the cleft of the active site of the enzymes for interaction.[112,113]

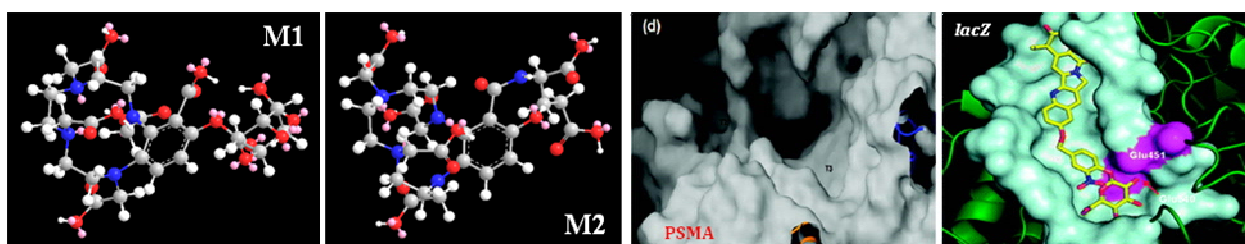
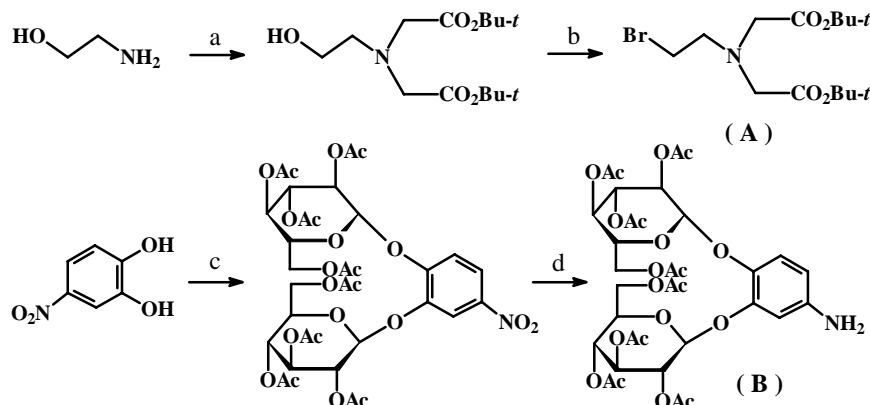


Figure 10

The molecular modeling and docking studies provide us a better understanding of the interactions between our designed target molecules and PSMA or *lacZ* proteins. We found that selecting a suitable structure with certain features (*e.g.* flexibility, linkage, appropriate angles, versatile binding modes, and coordination to Fe^{3+} with plastic chelating geometry) is crucial to the construction of the enzyme responsive enhanced MRI contrast agents. We also realized that the previous design and synthesis involved too many steps of reactions, not briefly and efficiently, displaying the increasing difficulty either in synthesis and purification with lower yields, especially, when the molecules grew bigger.

With these considerations in mind, we tried to introduce diethylenetriamine-*N,N',N'',N''*-tetraacetate (DTTA) instead of the cyclic DOTA or PCTA as $\text{Gd}(\text{III})$ chelator (see **Figure 11**) with a straightforward strategy. Most importantly, molecule M_9 can be hydrolyzed by β -galactosidase E801A in the presence of FAC in PBS (0.1 M, pH=7.4), producing obvious MRI contrast change before and after reaction with β -galactosidase E801A (see **Figure 12**), implying we found the right way. Inspired by these results, we extended this strategy further for the synthesis of other new molecules by using the Fe-chelation agents in anticancer therapy as the Fe-chelator for construction of the responsive MRI contrast agents. We firstly proved that the clinically applied Fe-chelators, such as Pyridoxal IsonicotinoylHydrazone (PIH), and its analogues Salicylaldehyde BenzoylHydrazone (SBH), Salicylaldehyde IsonicotinoylHydrazone (SIH) and Salicylaldehyde NicotinoylHydrazone (SNH), can act as

Fe-based ^1H MRI contrast agents to produce strong T_1 -weighted contrast effects (**Figure 13**, **TABLE 2**), suggesting that the Fe-complex formation could not only localize, accumulate and restrict the motion of the linked Gd-based ^1H MRI moiety, but also itself can produce the additional relaxivity.



Reaction Conditions: (a) $\text{BrCH}_2\text{CO}_2\text{Bu-}t$, KHCO_3 , 88%; (b) Ph_3P , NBS , 86%; (c) 2,3,4,6-tetra-*O*-acetyl- α -D-galactopyranosyl bromide, $\text{Hg}(\text{CN})_2$, 4Å M.S., CH_2Cl_2 , 92%; (d) H_2 , Pd/C , 100%.

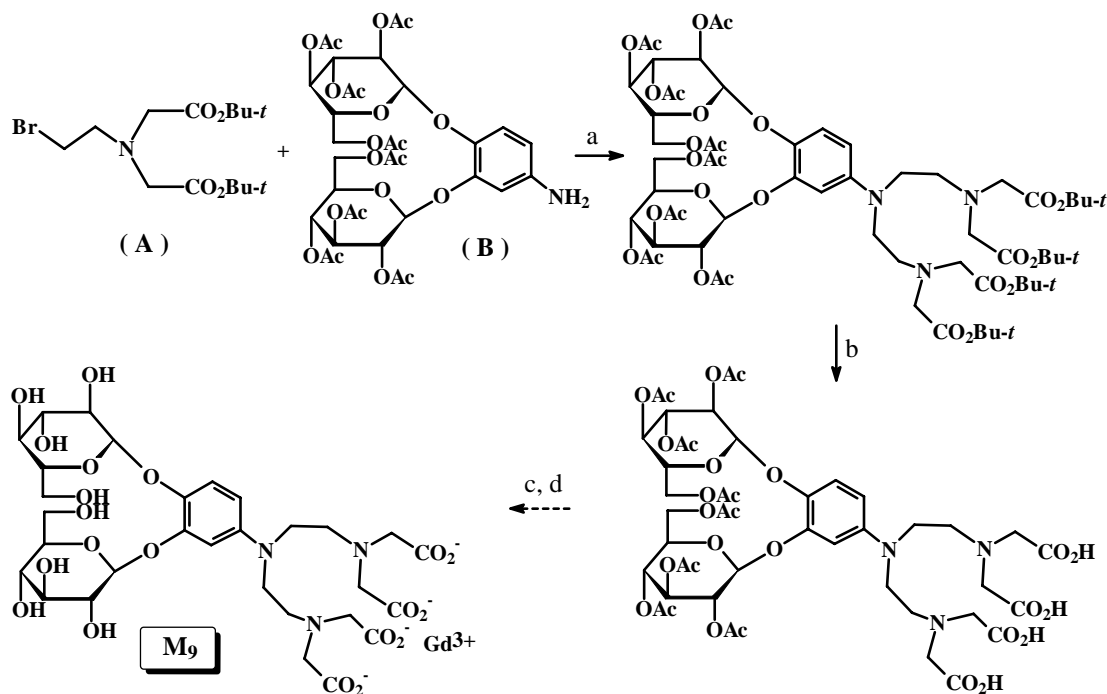


Figure 11. Reaction Conditions: (a) K_2CO_3 , MeCN , 78%; (b) $\text{CF}_3\text{CO}_2\text{H}$, CH_2Cl_2 , 84%; (c) GdCl_3 , Pyridine, 80%; (d) MeOH , MeONa , 86%.

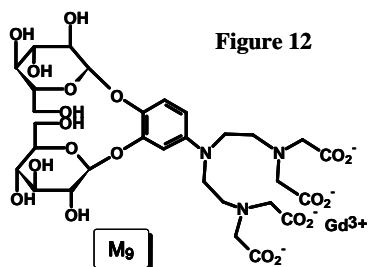


Figure 12

Figure 12. T_1 -weighted (TR/TE 250/12 ms) MR images of solutions and the signal intensity in test tubes at 4.7 T MR scanner: (A) PBS with **M9** and FAC; (B) PBS with **M9**, FAC and β -galactosidase E801A.



W

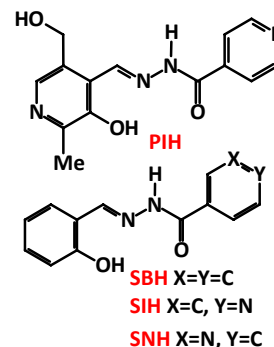


Figure 13

(u, Jian-Xin

Then, we synthesized M_{10} , M_{11} and M_{12} by using SBH, SIH and SNH as the Fe-chelators (see **Figure 14**). The MRI evaluation of the reporter molecules M_{10} , M_{11} and M_{12} , respectively, in sodium phosphate buffer solution (PBS) (0.1 M, pH=7.4) in the presence of ferric ammonia citrate (FAC) with β -galactosidase E801A indicated that: (1) Again, the reporter molecule M_{10} , similarly like M_9 , can be hydrolyzed by β -galactosidase E801A, producing apparent MRI contrast change upon response to β -galactosidase E801A; (2) Unlike M_9 and M_{10} , M_{11} and M_{12} have no MRI contrast enhancements with galactosidase E801A in the presence of FAC in PBS (0.1 M, pH=7.4), but with strong MRI contrast changes with galactosidase G5160 in the presence of FAC in PBS (0.1 M) at pH=4.5 (**Table 3**).

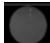

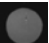









Chelator	PIH	SBH	SIH	SNH
T_1 -weighted ^1H MRI (Control) ¹				
T_1 -weighted ^1H MRI (Control) ²				
T_1 -weighted ^1H MRI (Complex)				

TABLE 2. (A) (1) Control, PIH, SBH, SIH or SNH each (1.6mM) in PBS; (2) Control, ferric ammonia citrate (FAC) (0.8mM) in PBS; (B) Complex, PIH, SBH, SIH or SNH each (1.6mM), FAC (0.8mM) in PBS; **CONDITIONS:** T_1 -weighted ^1H MRI, 200MHz, TR=300ms, TE =20ms, 1.5mm slice, 128×128, 50×50mm².

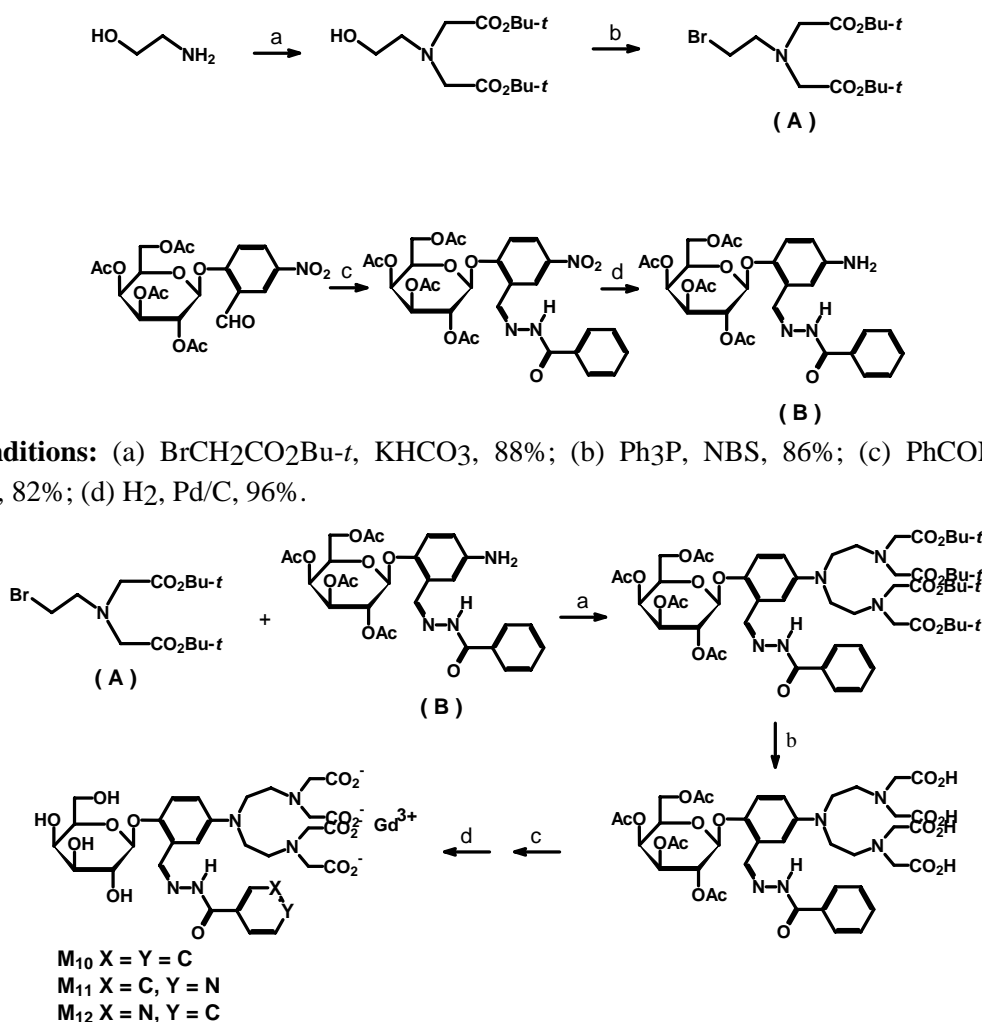

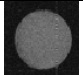
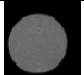
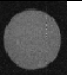
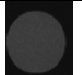
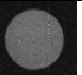

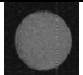
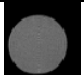

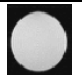

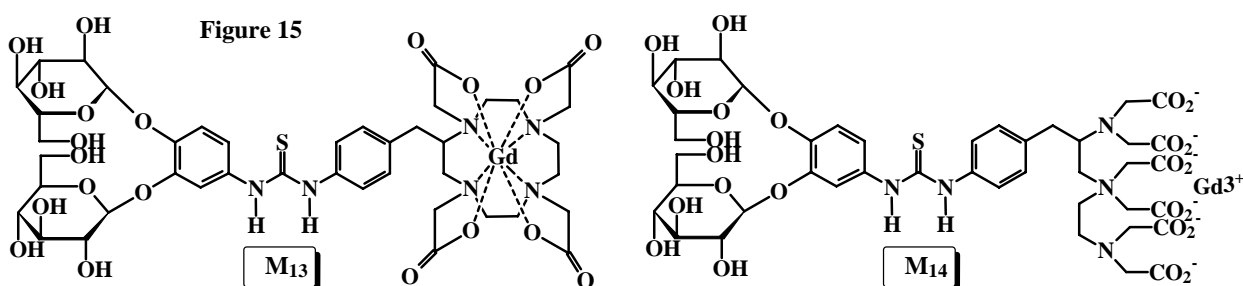


Table 3. ¹H-MRI contrast of the reporters **M**₁₀~**M**₁₂ in the presence of FAC with E801A in PBS (0.1M, pH=7.4) or G5160 in PBS (0.1M, pH=4.5). [Conditions: T₁-weighted ¹H MRI, 200MHz, TR=300ms, TE=20ms, 1.5mm slice, 128×128, 50×50mm². (A) Control, **M**₁₀~**M**₁₂ each (5μmol), FAC (2.5μmol), PBS (0.1M, pH=7.4, 1.5mL); (B) Complex, **M**₁₀~**M**₁₂ each (5μmol), FAC (2.5μmol), E801A (10 units), PBS (0.1M, pH=7.4, 1.5mL)], or G5160 (10 units), PBS (0.1M, pH=4.5, 1.5mL)].

Enzyme	β-galactosidase E801A			β-galactosidase G5160		
Molecule	M ₁₀	M ₁₁	M ₁₂	M ₁₀	M ₁₁	M ₁₂
T ₁ -weighted ¹ H MRI (Control)						
T ₁ -weighted ¹ H MRI (Enzyme)						

The experience accumulated on the development of enzyme responsive enhanced MRI contrast agents opened our mind, and the desire for an ideal *in vivo* MRI probe prompted us to design and syntheses another two kinds MRI agents: (1) through phenylthioureido as linkage connecting Gd³⁺ and Fe³⁺ chelators for suitable flexibility of the molecules **M**₁₃ and **M**₁₄ (see **Figure 15**), both like **M**₉ produced apparent MRI contrast differences upon response to β-galactosidase E801A.



(2) “Click Chemistry” Approach Because of regioselectivity, high yields in reasonable reaction times under mild conditions, “Click Chemistry” has been applied in a wide range of fields from synthetic chemistry to biomedicine and materials science. Our attention is on the versatile triazole rings as linkers between Fe³⁺ and Gd³⁺-ligands to functionalize with tolerance for the interaction with *lacZ* protein (see **Figure 16**).

In Vitro MRI Studies (1) **Cell preparation** (a) Stably transfected PC3 cell line: *E. coli lacZ* gene (from pSV-β-gal vector, Promega, Madison, WI) was inserted into high expression human cytomegalovirus (CMV) immediate-early enhancer/promoter vector phCMV (Gene Therapy Systems, San Diego, CA) giving a recombinant vector phCMV/*lacZ*, which was used to transfect PC3 cells using GenePORTER2 (Gene Therapy Systems). Cells were grown in DMEM (Dulbecco's Modification of Eagle's Medium, Mediatech, Inc, Herndon, VA), 10% FBS (Fetal bovine serum, Hyclone, Logan, UT) with 1% Penicillin-streptomycin Solution (Mediatech). The highest β-gal expressing colony was selected using G-418 disulfate (C₂₀H₄₀N₄O₁₀ · 2H₂SO₄, Research Products International Corp, Mt. Prospect, IL) (800 μg/ml), which was also included for routine culture (200 μg/ml). with 1% Penicillin-streptomycin Solution (Mediatech). The highest β-gal expressing colony was selected using G-418 disulfate

($\text{C}_{20}\text{H}_{40}\text{N}_4\text{O}_{10} \cdot 2\text{H}_2\text{SO}_4$, Research Products International Corp, Mt. Prospect, IL) (800 $\mu\text{g}/\text{ml}$), which was also included for routine culture (200 $\mu\text{g}/\text{ml}$).

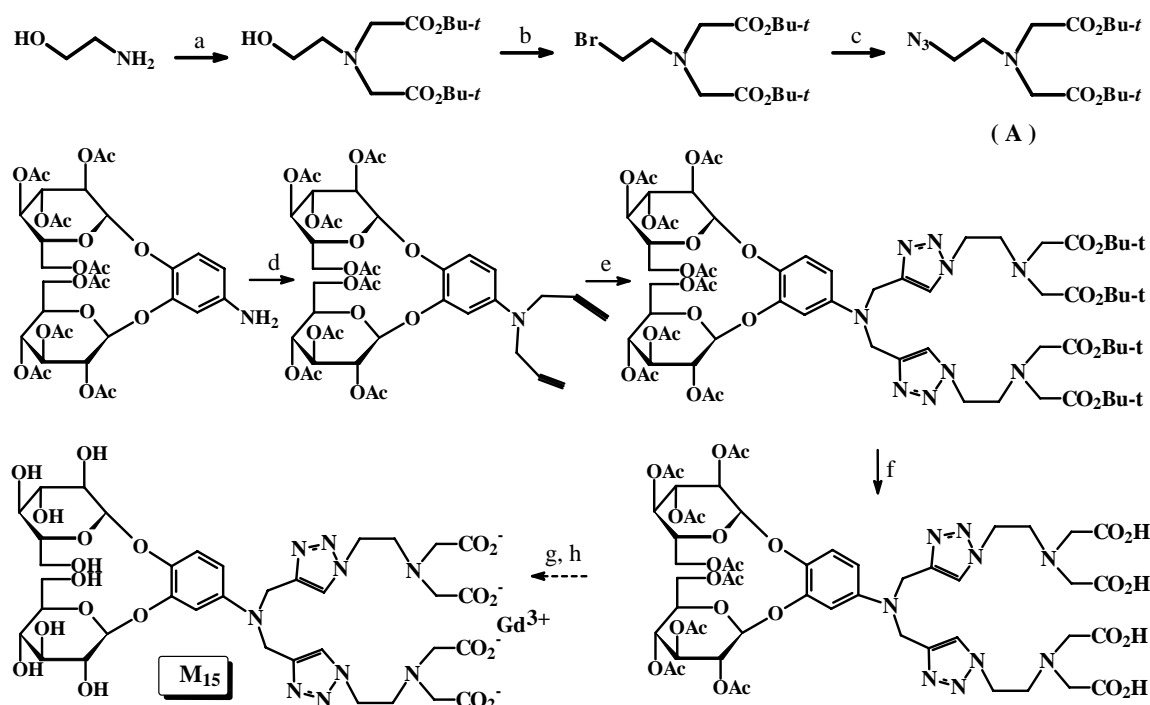


Figure 16. Reaction Conditions: (a) $\text{BrCH}_2\text{CO}_2\text{Bu-t}$, KHCO_3 , 88%; (b) Ph_3P , NBS, 86%; (c) NaN_3 , DMF, 80°C, 88%; (d) CHCCH_2Br , K_2CO_3 , DMF, rt, 86%; (e) (A), CuSO_4 , NaAsc, t-BuOH, rt, 69%; (f) $\text{CF}_3\text{CO}_2\text{H}$, CH_2Cl_2 , 74%; (g) GdCl_3 , Pyridine, 71%; (h) MeOH, MeONa, 82%.

(b) X-gal and S-gal staining for β -gal: cells were fixed in PBS plus 0.5% glutaraldehyde (5 min) and rinsed in PBS prior to staining. Staining was performed using standard procedures for 2 hours at 37 °C in PBS plus 1 mg/ml X-gal (Sigma, St. Louis, MO), 1 mM MgCl_2 , 5 mM $\text{K}_3\text{Fe}(\text{CN})_6$, and 5 mM $\text{K}_4\text{Fe}(\text{CN})_6$ or with 1.5 mg/ml S-gal (Sigma) and 2.5 mg/ml FAC (see Figure 17). (c) β -Gal activity assay: The β -gal activity of tumor cells and tissues in mice was measured using the β -gal assay kit (Promega, Madison, WI) with yellow *o*-

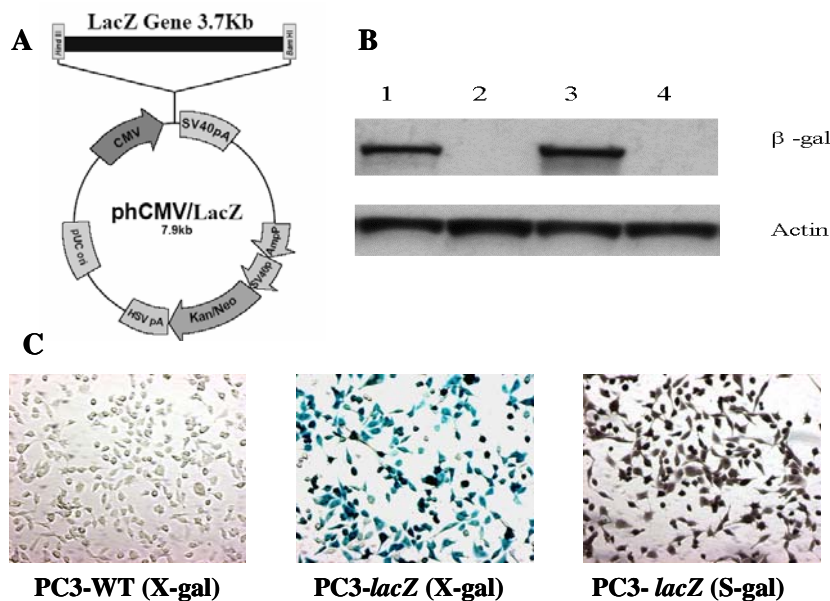


Figure 17 Generation of PC3 cells stably expressing of β -gal. (A) Map of recombinant *lacZ* vector (phCMV/*lacZ*). (B) Western blot: cell extracts of two transfected lines PC3-lacZ1 (lane 1) and PC3-lacZ (lane 3), together with PC3-WT (lanes 2 and 4) were examined. (C) PC3 wild-type and PC3-lacZ cells were stained using X-gal and S-gal: over 90% of PC3-lacZ cells were stained blue or black, respectively, while the PC3 wild type cells did not stain.

nitrophenyl β -D-galactopyranoside. (d) Western blot analysis: Protein was extracted from PC3 tumor cells and was quantified by a protein assay (Bio-Rad, Hercules, CA) based on the Bradford method. Each well was loaded with 30 μ g protein and separated by 10% SDS-PAGE (Nu-PAGE) and transferred to a polyvinylidene fluoride (PVDF) membrane. Primary monoclonal anti- β -gal antibody (Promega) and anti-actin antibody (Sigma) were used as probes at a dilution of 1:5000, and reacting protein was detected using a horseradish peroxidase-conjugated secondary antibody and ECL detection (Amersham, Piscataway, NJ).

(2) *In Vitro* MRI The *in vitro* evaluation of **M₉**~**M₁₄** with PC3-*lacZ* cells in the presence of FAC showed that only molecules **M₉** and **M₁₀** exhibited apparent MRI differences. **M₉** and **M₁₀** (6 μ mol) each in 1:1 DMSO/PBS was added to suspensions of 5 \times 10⁶ PC3 wild type and PC3-*lacZ* cells in PBS (1.0 mL) and FAC (3 μ mol) in wells and maintained at 37°C. MRI experiments were performed on a 4.7 T Varian Unity INOVA spectrometer. **Figure**

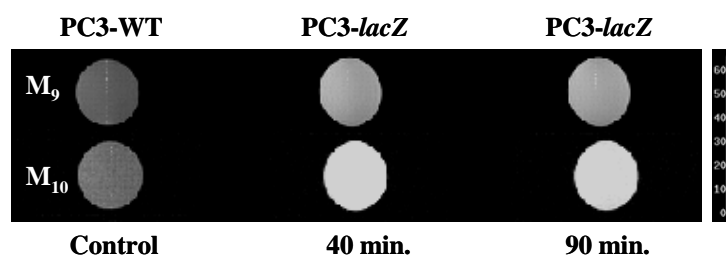


Figure 18 ¹H MRI, 200 MHz, TR=300ms, TE=20ms, 1.5mm slice, 128 \times 64, 40 \times 40 mm². (A) control, **M₉** or **M₁₀** (6 μ mol), FAC (3 μ mol), 5 \times 10⁶ PC3 WT, PBS (0.9 mL), DMSO (0.1 mL); (B) **M₉** or **M₁₀** (6 μ mol), FAC (3 μ mol), 5 \times 10⁶ PC3-*lacZ*, PBS (0.9 mL), DMSO (0.1 mL)].

18 showed the *in vitro* MR images of **M₉** and **M₁₀** with *lacZ* transfected prostate tumor cells, yielding obvious MRI contrast changes between in WT and *lacZ* transfected PC3 prostate tumor cells, indicating that both **M₉** and **M₁₀** can penetrate prostate tumor PC3 cell membrane and have no apparent cytotoxicity and no physiological perturbation effects on WT and *lacZ* transfected PC3 cells, the others **M₁₁**~**M₁₄** cannot cross prostate tumor PC3 cell membrane.

In Vivo* MRI Studies of **M₉** and **M₁₀* (1) **Animal model** All *in vivo* MRI studies were performed with approval from the Institutional Animal Care and Use Committee (IACUC). Wild type and stably transfected *lacZ* PC3 cells (2 \times 10⁶) were implanted subcutaneously in the left and right thighs of mice, respectively, when the tumors reached ~0.8 cm in diameter, the mouse was anesthetized (1.3% isoflurane/air at 1 dm³/min) with a facemask and maintained at 37°C by a warm pad with circulating water, and placed into animal coil for imaging. MRI data were acquired using a 4.7 T horizontal bore magnet with a Varian INOVA Unity system (Palo Alto, CA, USA). *T₁* and *T₂* values were measured using a spin echo sequence with varying repetition and echo times, e.g. *T₁*-weighted ¹H MRI, 200MHz, TR=0.2, 0.3, 0.5, 0.8, 1, 1.5, 2, 4, 6s, TE=12ms, 1.5mm slice, matrix=128 \times 128, FOV=50 \times 50mm²; *T₂*-weighted ¹H MRI, 200MHz, TR=6s, TE=11, 15, 20, 30, 50, 100, 150ms, 1.5mm slice, matrix=128 \times 128, FOV=50 \times 50mm². Histology analysis confirmed that PC3-*lacZ* tumor section showed over 90% of tissue stained blue for β -gal, while PC3-WT tumor histological section showed little or no blue stain (**Figure 19**). (2) ***In Vivo* MRI with i.v. injection** Mice bearing PC3-WT and PC3-*lacZ* tumors were imaged on a 4.7 T Varian Unity INOVA spectrometer. *T₁*-weighted transaxial images were obtained before and after intravenous injection of the

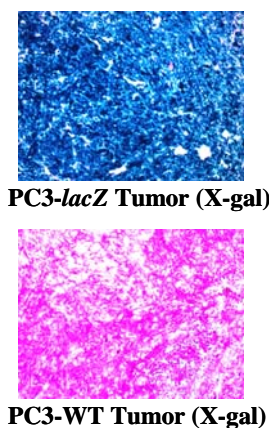


Figure 19

mixture of 0.4 mmol/kg **M**₉ and **M**₁₀ and FAC. Postcontrast scans were obtained every 15 min for one and half hours. For both reporters **M**₉ and **M**₁₀, the MR images of animals showed that there are no time-signal intensity changes between PC3-WT and PC3-*lacZ* tumors before and after **M**₉ and **M**₁₀ injection (**Figure 20**), indicating that both **M**₉ and **M**₁₀ can either be washed out or metabolized very quickly, and can't reach to PC3-WT and PC3-*lacZ* tumors on the thighs with enough amount. Also, we found that mice all died one and half-hours later after intravenous injection of **M**₉. **(3) In Vivo MRI with direct injection into tumors**

However, if a solution of **M**₁₀ (0.4 mmol/kg) and FAC (DMSO/PBS 1:1 V/V') was injected directly into the tumors

in a “fan” pattern, strong contrast was detected in the *lacZ* expressing PC3 tumors (**Figure 21**).

RESEARCH ACCOMPLISHMENTS

(1) Designed and synthesized a series of reporter molecules, and verified their structures, importantly, accumulated solid foundation, experience and expertise for the further investigation on molecular imaging.

(2) Finished the *in vitro* and *in vivo* evaluation of the reporter molecules **M**₉ and **M**₁₀, and the results demonstrated this novel mechanism proposed in W81XWH-05-1-0593 for imaging and evaluation of prostate cancer gene therapy is reliable.

REPORTABLE OUTCOMES

(1) A series of abstracts had been accepted for presentation on the various conferences such as World Molecular Imaging Congress, *Innovative Minds in Prostate Cancer Today*, American Chemical Society Meeting.

(2) Several papers are in preparation.

CONCLUSIONS

Prostate cancer is the most commonly diagnosed cancer and the second most common cause of cancer death in men in the United States. The advent of effective screening measures can sharply decrease the mortality of prostate cancer through detecting this disease at an earlier stage. However, the evidence for mortality benefit from prostate cancer screening has been disappointing to date. Expanding knowledge of prostate cancer biology with combination of imaging technologies would be of considerable value in many ongoing and future clinical prostate cancer diagnosis and gene therapy trials.

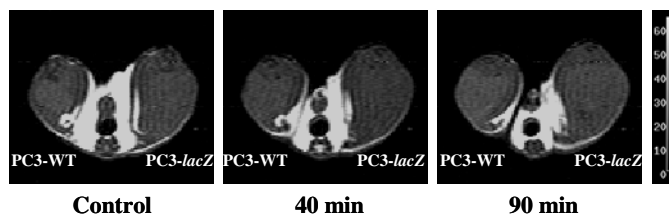


Figure 20 ¹H MRI, 200 MHz, TR=250ms, TE=12ms, 1.5mm slice, 128×64, 40×40 mm². (A) control; (B) **M**₁₀ (0.4 mmol/kg), FAC (0.2 mmol/kg), PBS/DMSO (1:1), i.v. injection].

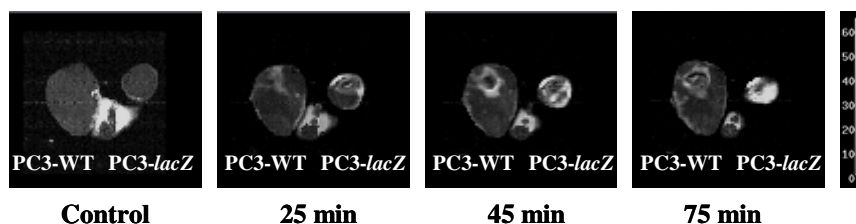


Figure 21 ¹H MRI, 200 MHz, TR=250ms, TE=12ms, 1.5mm slice, 128×64, 40×40 mm². (A) control; (B) **M**₁₀ (0.4 mmol/kg), FAC (0.2 mmol/kg), PBS/DMSO (1:1), i.v. injection].

Prostate Cancer Evaluation: Design, Synthesis and Evaluation of Novel Enzyme-Activated ¹H MRI Contrast Agents

Based on the biologic features of prostate cancer, we proposed in this project a new approach for *in vivo lacZ* gene expression assay or *in vivo* prostate cancer imaging. The ultimate objective is to demonstrate the utility and reliability of this new approach to measure β -gal or PSMA activities *in vivo*. We have accomplished a series of target molecules **M₁~M₁₄**, and verified by NMR data. Strong MRI contrast changes of target molecules **M₉** and **M₁₀** for detection *lacZ in vitro* and *in vivo* demonstrated this novel mechanism described in W81XWH-05-1-0593 is feasible and reliable. With screening out the ideal reporter molecules, we believe the translation of this novel approach to clinical investigations will enable prostate cancer detection comprehensive and infallible.

REFERENCES

1. American Cancer Society, Cancer Facts and Figures, 2009. (www.cancer.org).
2. Jemal A, Thomas A, Murray T, Thun M, 2002 Cancer statistics, 2002, *CA Cancer J. Clin.*, **52**, 23-47.
3. (a) Eastham JA, Hall SJ, Sehgal I, Wang J, Timme TL, Yang G, Connell-Crowley L, Elledge SJ, Zhang WW, Happer JW, 1995, *In vivo* gene therapy with p53 or p21 adenovirus for prostate cancer, *Cancer Res.*, **55**, 5151-5155; (b) Eastham JA, Chen SH, Sehgal I, Yang G, Timme TL, Hall SJ, Woo SL, Thompson TC, 1996, Prostate cancer gene therapy: Herpes simplex virus thymidine kinase gene transduction followed by ganciclovir in mouse and human prostate cancer models. *Hum. Gene Ther.*, **7**, 515-523.
4. Dorai T, Olsson CA, Katz AE, Buttyan R, 1997, Development of a hammerhead ribozyme against bcl-2. I. Preliminary evaluation of a potential gene therapeutic agent for hormonerefractory human prostate cancer, *Prostate*, **32**, 246-258.
5. Vieweg J, Rosenthal FM, Bannerji R, Heston WD, Fair WR, Gansbacher B, Gilboa E, 1994, Immunotherapy of prostate cancer in the Dunning rat model: Use of cytokine gene modified tumor vaccines. *Cancer Res.*, **54**, 1760-1765.
6. Sokoloff MH, Tso CL, Kaboo R, Taneja S, Pang S, Dekernion JB, Belldegrun AS, 1996, In vitro modulation of tumor progression-associated properties of hormone refractory prostate carcinoma cell lines by cytokines, *Cancer*, **77**, 1862-1872.
7. Simons JW, Mikhak B, Chang JF, Demarzo AM, Carducci MA, Lim M, Weber CE, Baccala AA, Goemann MA, Clift SM, Ando DG, Levitsky HI, Cohen LK, Sanda MG, Mulligan RC, Partin AW, Carter HB, Piantadosi S., Marshall FF, Nelson WG, 1999, Induction of immunity to prostate cancer antigens: Results of a clinical trial of vaccination with irradiated autologous prostate tumor cells engineered to secrete granulocytemacrophage colony-stimulating factor using *ex vivo* gene transfer. *Cancer Res.*, **59**, 5160-5168.
8. Belldegrun A, Tso CL, Zisman A, Naitoh J, Said J, Pantuck AJ, Hinkel A, Dekernion J, Figlin R, 2001, Interleukin 2 gene therapy for prostate cancer: Phase I clinical trial and basic biology, *Hum. Gene Ther.*, **12**, 883-892.
9. Blackburn RV, Galoforo SS, Corry PM, Lee YJ, 1998, Adenoviral-mediated transfer of a heat-inducible double suicide gene into prostate carcinoma cells. *Cancer Res.*, **58**, 1358-362.
10. Pantuck AJ, Matherly J, Zisman A, Nguyen D, Berger F, Gambhir SS, Black ME, Belldegrun A, Wu L, 2002, Optimizing Prostate Cancer Suicide Gene Therapy Using Herpes Simplex Virus Thymidine Kinase Active Site Variants, *Hum. Gene Ther.*, **13**, 777-789.
11. Igawa T, Lin FF, Rao P, Lin MF, 2003, Suppression of LNCaP prostate cancer xenograft tumors by a prostate-specific protein tyrosine phosphatase, prostatic acid phosphatase, *Prostate*, **55**, 247-258.
12. Steiner MS, Gingrich JR, 2000, Gene therapy for prostate cancer: Where are we now? *J. Urol.*, **164**, 1121-1136.
13. Harrington KJ, Spitzweg C, Bateman AR, Morris JC, Vile RG, 2001, Gene therapy for prostate cancer: Current status and future prospects, *J. Urol.*, **166**, 1220-1233.
14. Morris MJ, Scher HI, 2000, Novel strategies and therapeutics for the treatment of prostate carcinoma, *Cancer*, **89**, 1329-1348.

15. Gardner TA, Sloan J, Raikwar SP, Kao C, 2002, Prostate Cancer Gene Therapy: Past Experiences and Future Promise, *Cancer and Metastasis Reviews*, **21**, 137-145.
16. Shalev M, Thompson TC, Kadmon D, Ayala G, Kernen K, Miles BJ, 2001, Gene therapy for prostate cancer, *Urology*, **57**, 8-16.
17. Gyorffy S, Palmer K, Gauldie J, 2001, Adenoviral vector expressing murine angiostatin inhibits a model of breast cancer metastatic growth in the lungs of mice, *Am. J. Path.*, **159**, 1137-47.
18. Yazawa, K, Fujimori M, Nakamura T, Sasaki T, Amano J, Kano Y, Taniguchi S, 2001, Bifidobacterium longum as a delivery system for gene therapy of chemically induced rat mammary tumors, *Cancer Res. Treat.*, **66**, 165-170.
19. Sato M, Johnson M, Zhang L, Zhang B, Le K, Gambhir SS, Carey M, Wu L, 2003, Optimization of adenoviral vectors to direct highly amplified prostate-specific expression for imaging and gene therapy, *Mol. Ther.*, **8**, 726-737.
20. Wu L, Sato M, 2003, Integrated, molecular engineering approaches to develop prostate cancer gene therapy, *Curr. Gene Ther.*, **3**, 452-467.
21. Bastide C, Maroc N, Bladou F, Hassoun J, Maitland N, Mannoni P, Bagnis C, 2003, Expression of a model gene in prostate cancer cells lentivirally transduced in vitro and in vivo, *Prostate Cancer and Prostatic Diseases*, **6**, 228-234.
22. Stanbridge LJ, Dussupt V, Maitland NJ, 2003, Baculoviruses as vectors for gene therapy against human prostate cancer, *J. Biomed. Biotech.*, **6**, 79-91.
23. Igawa T, Lin F, Rao P, Lin M, 2003, Suppression of LNCaP prostate cancer xenograft tumors by a prostate-specific protein tyrosine phosphatase, prostatic acid phosphatase, *Prostate*, **55**, 247-258.
24. Nasu Y, 2002, Prostate cancer gene therapy: current status of clinical trial, *Igaku no Ayumi*, **203**, 323-327.
25. Pantuck AJ, Berger F, Zisman A, Nguyen D, Tso C, Matherly J, Gambhir SS, Beldegrun AS, 2002, CL1-SR39: a noninvasive molecular imaging model of prostate cancer suicide gene therapy using positron emission tomography, *J. Urology*, **168**, 1193-1198.
26. Kaminski JM, Nguyen K, Buyyounouski M, Pollack A, 2002, Prostate cancer gene therapy and the role of radiation, *Cancer Treatment Rev.*, **28**, 49-64.
27. Gdor Y, Timme TL, Miles BJ, Kadmon D, Thompson TC, 2002, Gene therapy for prostate cancer, *Expert Review of Anticancer Therapy*, **2**, 309-321.
28. Pantuck AJ, Matherly J, Zisman A, Nguyen D, Berger F, Gambhir SS, Black ME, Beldegrun A, Wu L, 2002, Optimizing prostate cancer suicide gene therapy using herpes simplex virus thymidine kinase active site variants, *Human Gene Therapy*, **13**, 777-789.
29. Zhang L, Adams JY, Billick E, Ilagan R, Iyer M, Le K, Smallwood A, Gambhir SS, Carey M, Wu L, 2002, Molecular engineering of a two-step transcription amplification (TSTA) system for transgene delivery in prostate cancer, *Mol. Ther.*, **5**, 223-232.
30. Voelkel-Johnson C, King DL, Norris JS, 2002, Resistance of prostate cancer cells to soluble TNF-related apoptosis-inducing ligand (TRAIL/Apo2L) can be overcome by doxorubicin or adenoviral delivery of full-length TRAIL, *Cancer Gene Therapy*, **9**, 164-172.

31. Pramudji C, Shimura S, Ebara S, Yang G, Wang J, Ren C, Yuan Y, Tahir SA, Timme TL, Thompson TC, 2001, *In situ* prostate cancer gene therapy using a novel adenoviral vector regulated by the caveolin-1 promoter, *Clinical Cancer Research*, **7**, 4272-4279.
32. Li Y, Okegawa T, Lombardi DP, Frenkel EP, Hsieh JT, 2002, Enhanced transgene expression in androgen independent prostate cancer gene therapy by taxane chemotherapeutic agents, *J. Urology*, **167**, 339-346.
33. Hsieh CL, Chung LWK, 2001, New perspectives of prostate cancer gene therapy: molecular targets and animal models, *Critical Reviews in Eukaryotic Gene Expression*, **11**, 77-120.
34. Serebriiskii IG, Golemis EA, 2000, Uses of *lacZ* to Study Gene Function: Evaluation of β -Galactosidase Assays Employed in the Yeast Two-Hybrid System, *Anal. Biochem.*, **285**, 1-15.
35. Sanes JR, Rubenstein JL, Nicolas JF, Use of a recombinant retrovirus to study post-implantation cell lineage in mouse embryos, *EMBO J.*, 1986, **5**, 3133-3142.
36. James AL, Perry JD, Chilvers K, Robson IS, Armstrong L, Orr KE, Alizarin- β -D-galactoside: a new substrate for the detection of bacterial β -galactosidase, *Lett. Appl. Microbiol.*, 2000, **30**, 336-340.
37. Aamlid KH, Lee G, Smith BV, Richardson AC, Price RG, New colorimetric substrates for the assay of glycosidases, *Carbohydr. Res.*, 1990, **205**, C5-C9.
38. Sanchez-Ramos J, Song S, Dailey M, Cardozo-Pelaez F, Hazzi C, Stedeford T, Willing A, Freeman TB, Saporta S, Zigova T, Sanberg PR, Snyder EY, The X-gal caution in neural transplantation studies, *Cell Transplant.*, 2000, **9**, 657-667.
39. Li L, Zemp RJ, Lungu G, Stoica G, Wang LV, Photoacoustic imaging of *lacZ* gene expression *in vivo*, *J. Biomed. Opt.*, 2007, **12**, 020504.
40. Rotman B, Zderic JA, Edelstein M, Fluorogenic substrates for β -D-galactosidases and phosphatases derived from fluorescein (3,6-dihydroxyfluoran) and its monomethylether, *Proc. Natl. Acad. Sci. U.S.A.*, 1963, **50**, 1-6.
41. Lo JT, Mukerji K, Awasthi YC, Hanada E, Suzuki K, Srivastava SK, Purification and properties of sphingolipid β -galactosidases from human placenta, *J. Biol. Chem.*, 1979, **254**, 6710-6715.
42. Nolan GP, Fiering S, Nicolas JF, Herzenberg LA, Fluorescence activated cell-analysis and sorting of viable mammalian cells based on β -D-galactosidase activity after transduction of *Escherichia coli lacZ*, *Proc. Natl. Acad. Sci. U.S.A.*, 1988, **85**, 2603-2607.
43. Zhang YZ, Naleway JJ, Larison KD, Huang Z, Haugland RP, Detecting *lacZ* gene expression in living cells with new lipophilic, fluorogenic β -galactosidase substrates, *FASEB J.*, 1991, **5**, 3108-3113.
44. Corey PF, Trimmer RW, Biddlecom WG, A new chromogenic β -galactosidase substrate: 7- β -D-galactopyranosyloxy-9,9-dimethyl-9H-acridin-2-one, *Angew. Chem., Int. Ed. Engl.*, 1991, **30**, 1646-1648.
45. Young DC, Kingsley SD, Ryan KA, Dutko FJ, Selective inactivation of eukaryotic β -galactosidase in assays for inhibitors of HIV-1 TAT using bacterial β -galactosidase as a reporter enzyme, *Anal. Biochem.*, 1993, **215**, 24-30.
46. Rakhmanova VA, MacDonald RC, A microplate fluorimetric assay for transfection of the β -galactosidase reporter gene, *Anal. Biochem.*, 1998, **257**, 234-237.
47. Gee KR, Sun WC, Bhalgat MK, Upson RH, Klaubert DH, Latham KA, Haugland RP, Fluorogenic substrates based on fluorinated umbelliferones for continuous assays of phosphatases and β -galactosidases, *Anal. Biochem.*, 1999, **273**, 41-48.

48. Chilvers KF, Perry JD, James AL, Reed RH, Synthesis and evaluation of novel fluorogenic substrates for the detection of bacterial β -galactosidase, *J. Appl. Microbiol.*, 2001, **91**, 1118-1130.
49. Tung CH, Zeng Q, Shah K, Kim DE, Schellingerhout D, Weissleder R, *In vivo* imaging of β -galactosidase activity using far red fluorescent switch, *Cancer Res.*, 2004, **64**, 1579-1583.
50. Urano Y, Kamiya M, Kanda K, Ueno T, Hirose K, Nagano T, Evolution of fluorescein as a platform for finely tunable fluorescence probes, *J. Am. Chem. Soc.*, 2005, **127**, 4888-4894.
51. Kamiya M, Kobayashi H, Hama Y, Koyama Y, Bernardo M, Nagano T, Choyke PL, Urano Y, An enzymatically activated fluorescence probe for targeted tumor imaging, *J. Am. Chem. Soc.*, 2007, **129**, 3918-3929.
52. Jossierand V, Texier-Nogues I, Huber P, Favrot MC, Coll JL, Non-invasive *in vivo* optical imaging of the *lacZ* and *luc* gene expression in mice, *Gene Therapy*, 2007, **14**, 1587-1593.
53. Ho NH, Weissleder R, Tung CH, A self-immolative reporter for β -galactosidase sensing, *ChemBioChem*, 2007, **8**, 560-566.
54. Takayasu S, Maeda M, Tsuji A, Chemiluminescent enzyme immunoassay using β -D-galactosidase as the label and the bis(2,4,6-trichlorophenyl)oxalate-fluorescent dye system, *J. Immunol. Methods*, 1985, **83**, 317-325.
55. Arakawa H, Maeda M, Tsuji A, Chemiluminescent assay of various enzymes using indoxyl derivatives as substrate and its applications to enzyme immunoassay and DNA probe assay, *Anal. Biochem.*, 1991, **199**, 238-242.
56. Jain VK, Magrath IT, A chemiluminescent assay for quantitation of β -galactosidase in the femtogram range: Application to quantitation of β -galactosidase in *lacZ*-transfected cells, *Anal. Biochem.*, 1991, **199**, 119-124.
57. Maeda M, Shimizu S, Tsuji A, Chemiluminescence assay of β -D-galactosidase and its application to competitive immunoassay for 17 α -hydroxyprogesterone and thyroxine, *Anal. Chim. Acta*, 1992, **266**, 213-217.
58. Beale EG, Deeb EA, Handley RS, Akhavan-Tafti H, Schaap AP, A rapid and simple chemiluminescent assay for *Escherichia coli* β -galactosidase, *Biotechniques*, 1992, **12**, 320-323.
59. Fulton R, Van Ness B, Luminescent reporter gene assays for luciferase and β -galactosidase using a liquid scintillation counter, *Biotechniques*, 1993, **14**, 762-763.
60. Dodeigne C, Thunus L, Lejeune R, Chemiluminescence as diagnostic tool, *Talanta*, 2000, **51**, 415-439.
61. Wehrman TS, von Degenfeld G, Krutzik PO, Nolan GP, Blau HM, Luminescent imaging of β -galactosidase activity in living subjects using sequential reporter-enzyme luminescence, *Nat. Methods*, 2006, **3**, 295-301.
62. Bormans G, Verbruggen A, Enzymatic synthesis and biodistribution in mice of β -O-D-galactopyranosyl-(1,4')-2'-[¹⁸F]fluoro-2'-deoxy-D-glucopyranose (2'-[¹⁸F]fluorodeoxylactose), *J. Labelled Compd. Radiopharm.*, 2001, **44**, 417-423.
63. Choi JH, Choe YS, Lee KH, Choi Y, Kim SE, Kim BT, Synthesis of radioiodine-labeled 2-phenylethyl 1-thio- β -D-galactopyranoside for imaging of *lacZ* gene expression, *Carbohydr. Res.*, 2003, **338**, 29-34.
64. Lee KH, Byun SS, Choi JH, Paik JY, Choe YS, Kim BT, Targeting of *lacZ* reporter gene expression with radioiodine-labelled phenylethyl- β -D-thiogalactopyranoside, *Eur. J. Nucl. Med. Mol. Imaging*, 2004, **31**, 433-438.
65. Celen S, Deroose C, de Groot T, Chitneni SK, Gijssbers R, Debyser Z, Mortelmans L, Verbruggen A, Bormans G, Synthesis and evaluation of ¹⁸F- and ¹¹C-labeled phenyl-galactopyranosides as potential probes for *in vivo*

- visualization of *lacZ* gene expression using positron emission tomography, *Bioconjugate Chem.*, 2008, **19**, 441-449.
66. Van Dort ME, Lee KC, Hamilton CA, Rebemtulla A, Ross BD, Radiosynthesis and evaluation of 5-[¹²⁵I]iodoindol-3-yl-β-D-galactopyranoside as a β-galactosidase imaging radioligand, *Mol. Imaging*, 2008, **7**, 187-197.
67. Moats RA, Fraser SE, Meade TJ, A "smart" magnetic resonance imaging agent that reports on specific enzyme activity, *Angew. Chem. Intl. Edn. Engl.*, 1997, **36**, 726-728.
68. Louie AY, Huber MM, Ahrens ET, Rothbacher U, Moats R, Jacobs RE, Fraser SE, Meade TJ, *In vivo* visualization of gene expression using magnetic resonance imaging, *Nature Biotechnol.*, 2000, **18**, 321-325.
69. Chang YT, Cheng CM, Su YZ, Lee WT, Hsu JS, Liu GC, Cheng TL, Wang YM, Synthesis and characterization of a new bioactivated paramagnetic gadolinium(III) complex [Gd(DOTA-FPG)(H₂O)] for tracing gene expression, *Bioconjugate Chem.*, 2007, **18**, 1716-1727.
70. Yu JX, Otten P, Ma ZY, Cui WN, Liu L, Mason RP, A novel NMR platform for *in vivo* detecting gene transfection: Synthesis and evaluation of fluorinated phenyl β-D-galactosides with potential application for *in vivo* assessing *lacZ* gene expression, *Bioconjugate Chem.*, 2004, **15**, 1334-1341.
71. Cui WN, Otten P, Li YM, Koeneman K, Yu JX, Mason RP, A novel NMR approach to assessing gene transfection: 4-fluoro-2-nitrophenyl-β-D-galactopyranoside as a prototype reporter molecule for β-galactosidase, *Magn. Reson. Med.*, 2004, **51**, 616-620.
72. Yu JX, Ma ZY, Li YM, Koeneman KS, Liu L, Mason RP, Synthesis and evaluation of a novel gene reporter molecule: detection of β-galactosidase activity using ¹⁹F NMR of a fluorinated vitamin B₆ conjugate, *Med. Chem.*, 2005, **3**, 255-262.
73. Yu JX, Kodibagkar VD, Cui WN, Mason RP, ¹⁹F: a versatile reporter for non-invasive physiology and pharmacology using magnetic resonance, *Curr. Med. Chem.*, 2005, **12**, 819-848.
74. Yu JX, Liu L, Kodibagkar VD, Cui WN, Mason RP, Synthesis and evaluation of novel enhanced gene reporter molecules: detection of β-galactosidase activity using ¹⁹F NMR of trifluoromethylated aryl β-D-galactopyranosides, *Bioorg. Med. Chem.*, 2006, **14**, 326-333.
75. Yu JX, Mason RP, Synthesis and characterization of novel *lacZ* gene reporter molecules: detection of β-galactosidase activity using ¹⁹F NMR of polyglycosylated fluorinated vitamin B₆, *J. Med. Chem.*, 2006, **49**, 1991-1999.
76. Kodibagkar VD, Yu JX, Liu L, Brown S, Hetherington HP, Mason RP, Imaging β-galactosidase activity using ¹⁹F CSI of *lacZ* gene-reporter molecule 2-fluoro-4-nitrophenol-β-D-galactopyranoside (OFPNPG), *Magn. Reson. Imaging*, 2006, **24**, 959-962.
77. Liu L, Kodibagkar VD, Yu JX, Mason RP, ¹⁹F-NMR detection of *lacZ* gene expression via the enzymic hydrolysis of 2-fluoro-4-nitrophenyl β-D-galactopyranoside *in vivo* in PC3 prostate tumor xenografts in the mouse, *FASEB J.*, 2007, **21**, 2014-2019.
- 78.. (a) Aime S, Geninatti Crich S, Gianolio E, Giovenzana GB, Tei L, Terreno E, 2006, High sensitivity lanthanide(III) based probes for MR-medical imaging, *Coordination Chem. Rev.*, **250**, 1562-1579; (b) Weissleder R, Moore A, Mahmood U, Bhorade R, Benveniste H, Chiocca EA, Basilion JP, 2000, *In vivo* magnetic resonance imaging of transgene expression, *Nature Medicine*, **6**, 351-354; (c) Weissleder R, Mahmood U, 2001, Molecular Imaging, *Radiology*, **219**, 316-333.

79. Caravan P, Ellison JJ, McMurry TJ, Lauffer RB, 1999, Gadolinium(III) chelates as MRI contrast agents: Structure, dynamics, and applications, *Chem. Rev.*, **99**, 2293-2352.
80. Comblin V, Gilsoul D, Hermann M, Humblet V, Jacques V, Mesbahi M, Sauvage C, Desreux JF, 1999, Designing new MRI contrast agents: A coordination chemistry challenge, *Coordination Chem. Rev.*, **185-186**, 451-470.
81. Lauffer RB, Parmelee DJ, Dunham S, Ouellet HS, Dolan RP, Witte S, McMurry TJ, Walovich RC, 1998, MS-325: albumin-targeted contrast agent for MR angiography, *Radiology*, **207**, 529-538.
82. Rudin M, Mueggler T, Allegrini PR, Baumann D, Rausch M, 2003, Characterization of CNS disorders and evaluation of therapy using structural and functional MRI, *Anal. Bioanal. Chem.*, **377**, 973-981.
83. Bell JD, Taylor-Robinson SD, 2000, Assessing gene expression *in vivo*: magnetic resonance imaging and spectroscopy, *Gene Therapy*, **7**, 1259-1264.
84. (a) Louie AY, Hüber MM, Ahrens ET, Rothbächer U, Moats R, Jacobs RE, Fraser SE, Meade TJ, 2000, *In vivo* visualization of gene expression using magnetic resonance imaging, *Nature Biotechnology*, **18**, 321-325; (b) Jacobs RE, Ahrens ET, Meade TJ, Fraser SE, 1999, Looking deeper into vertebrate development, *Cell Biology*, **9**, 73-76; (c) Moats RA, Fraser SE, Meade TJ, 1997, A "smart" magnetic resonance imaging agent that reports on specific enzyme activity, *Angew. Chem. Intl. Edn. Engl.*, **36**, 726-728.
85. (a) Jacques V, Desreux JF, 2002, New classes of MRI contrast agents, *Topics Curr. Chem.*, **221**, 123-164; (b) Jacques V, Desreux JF, 2001, Synthesis of MRI contrast agents. II. Macrocyclic ligands, *Chemistry of Contrast Agents in Medical Magnetic Resonance Imaging*, 157-191.
86. (a) Ruloff R, van Koten G, Merbach AE, Novel heteroditopic chelate for self-assembled gadolinium(III) complex with high relaxivity, *Chem. Comm.*, **2004**, (7), 842-843; (b) Costa J, Ruloff R, Burai L, Helm L, Merbach AE, Rigid M^{II}L₂Gd₂^{III} (M = Fe, Ru) Complexes of a Terpyridine-Based Heteroditopic Chelate: A Class of Candidates for MRI Contrast Agents, *J. Am. Chem. Soc.*, **2005**, **127**, 5147-5157; (c) Livramento JB, Tóth É, Sour A, Borel A, Merbach AE, Ruloff R, High Relaxivity Confined to a Small Molecular Space: A Metallostar-Based, Potential MRI Contrast Agent, *Angew. Chem.*, **2005**, **44**, 1480-1484; (d) Torres S, Martins JA, André JP, Geraldes CFGC, Merbach AE, Tóth É, Supramolecular Assembly of an Amphiphilic Gd^{III} Chelate: Tuning the Reorientational Correlation Time and the Water Exchange Rate, *Chem. Eur. J.*, **2006**, **12**, 940-948. (e) Helm L, Merbach AE, Inorganic and Bioinorganic Solvent Exchange Mechanisms, *Chem. Rev.*, **2005**, **105**, 1923-1960.
87. (a) Livramento JB, Toth E, Sour A, Borel A, Merbach AE, Ruloff R, High relaxivity confined to a small molecular space: A metallostar-based, potential MRI contrast agent, *Angew. Chem.*, **2005**, **44**, 1480-1484; (b) Torres S, Martins JA, Andre JP, Geraldes CFGC, Merbach AE, Toth E, Supramolecular assembly of an amphiphilic Gd^{III} chelate: Tuning the reorientational correlation time and the water exchange rate, *Chem. Eur. J.*, **2006**, **12**, 940-948;
88. Livramento JB, Sour A, Borel A, Merbach AE, Toth E, A starburst-shaped heterometallic compound incorporating six densely packed Gd³⁺ ions, *Chem. Eur. J.*, **2006**, **12**, 989-1003.
89. (a) Faa G., Crisponi G. (1999). Iron chelating agents in clinical practice. *Coordinat. Chem. Rev.* **184**, 291-310; (b) Richardson D. R. (1999). The therapeutic potential of iron chelators. *Expert Opin. Investigational Drugs* **8**, 2141-2158; (c) Richardson D. R. (2002). Iron chelators as therapeutic agents for the treatment of cancer. *Critical Rev. Oncology/Hematology* **42**, 267-281; (d) Zu D., Hider

- R. C. (2002). Design of iron chelators with therapeutic application. *Coordinat. Chem. Rev.* 232, 151-171; (e) Le N. T. V., Richardson D. R. (2002). The role of iron in cell cycle progression and the proliferation of neoplastic cells. *Biochim. Biophys. Acta* 1603, 31-46; (f) Richardson D. R. (2002). Therapeutic potential of iron chelators in cancer therapy. *Adv. Exp. Med. Biology* 509, 231-249; (g) Buss J. L., Torti F. M., Torti S. V. (2003). The role of iron chelation in cancer therapy. *Curr. Med. Chem.* 10, 1021-1034; (h) Kontoghiorghes G. J., Pattichis K., Neocleous K., Kolnagou A. (2004) The design and development of deferiprone (L1) and other iron chelators for clinical use: Targeting methods and application prospects. *Curr. Med. Chem.* 11, 2161-2183; (i) Buss J. L., Greene B. T., Turner J., Torti F. M., Torti S. V. (2004). Iron chelators in cancer chemotherapy. *Curr. Topics Med. Chem.* 4, 1623-1635; (j) Richardson D. R. (2005). Molecular mechanisms of iron uptake by cells and the use of iron chelators for the treatment of cancer. *Curr. Med. Chem.* 12, 2711-2729; (k) Kalinowski D. S., Richardson D. R. (2005). The Evolution of Iron Chelators for the Treatment of Iron Overload Disease and Cancer. *Pharmacol. Rev.* 57, 547-583; (l) Birch N., Wang X., Chong H. S. (2006). Iron chelators as therapeutic iron depletion agents. *Expert Opin. Therap. Patients* 16, 1533-1556; (m) Richardson D. R., Sharpe P. C., Lovejoy D. B., Senaratne D., Kalinowski D.S., Islam M., Bernhardt P. V. (2006). Dipyrindyl thiosemicarbazone chelators with potent and selective antitumor activity form iron complexes with redox activity. *J. Med. Chem.* 49, 6510-6521; (n) Kalinowski D. S., Yu Y., Sharpe P. C., Islam M., Liao Y. T., Lovejoy D. B., Kumar N., Bernhardt P. V., Richardson D. R. (2007). Design, synthesis, and characterization of novel iron chelators: Structure–activity relationships of the 2-benzoylpyridine thiosemicarbazone series and their 3-nitrobenzoyl analogues as potent antitumor agents. *J. Med. Chem.* 50, 3716-3729; (o) Yuan J., Lovejoy D. B., Richardson D. R. (2004). Novel di-2-pyridyl-derived iron chelators with marked and selective antitumor activity: in vitro and in vivo assessment. *Blood* 104, 1450-1458; (p) Chong H. S., Ma X., Lee H., Bui P., Song H. A., Birch N. (2008). Synthesis and Evaluation of Novel Polyaminocarboxylate-Based Antitumor Agents. *J. Med. Chem.* 51, 2208-2215; (q) Assinder S. J., Dong Q., Mangs H., Richardson D. R. (2009). Pharmacological Targeting of the Integrated Protein Kinase B, Phosphatase and Tensin Homolog Deleted on Chromosome 10, and Transforming Growth Factor- β Pathways in Prostate Cancer. *Mol. Pharmacol.* 75, 429-436; (r) Rao V. A., Klein S. R., Agama K. K., Toyoda E., Adachi N., Pommier Y., Shacter E. B. (2009). The Iron Chelator Dp44mT Causes DNA Damage and Selective Inhibition of Topoisomerase II α in Breast Cancer Cells. *Cancer Res.* 69, 948-957.
90. Abeyasinghe R. D., Greene B. T., Haynes R., Willingham M. C., Turner J., Planalp R. P., Brechbiel M. W., Torti F. M., Torti S. V. (2001). p53-independent apoptosis mediated by tachpyridine, an anti-cancer iron chelator. *Carcinogenesis* 22, 1607-1614.
91. Faulk W. P., His B. L., Stevens P.J. (1980). Transferrin and transferrin receptors in carcinoma of the breast. *Lancet* 2, 390–392.
92. Seymour G. J., Walsh M. D., Lavin M. F., Strutton G., Gardiner R. A. (1987). Transferrin receptor expression by human bladder transitional cell carcinomas. *Urol. Res.* 15, 341-344.

93. Becker E. M., Lovejoy D. B., Greer J. M., Watts R., Richardson D. R. (2003). Identification of the di-pyridyl ketone isonicotinoyl hydrazone (PKIH) analogues as potent iron chelators and anti-tumour agents. *Br. J. Pharmacol.* 138, 819-830.
94. Hershko C. (1994). Control of disease by selective iron depletion: a novel therapeutic strategy utilizing iron chelators. *Baillière's Clin. Haematol.* 7, 965-100.
95. (a) Le N. T. V., Richardson D. R. (2004). Iron chelators with high antiproliferative activity up-regulate the expression of a growth inhibitory and metastasis suppressor gene: a link between iron metabolism and proliferation. *Blood* 104, 2967-2975; (b) Yu Y., Wong J., Lovejoy D. B., Kalinowski D. S., Richardson D. R. (2006). Chelators at the Cancer Coalface: Desferrioxamine to Triapine and Beyond. *Clin. Cancer Res.* 12, 6876-6883.
96. (a) Lovejoy D. B., Richardson D. R. (2003) Iron chelators as anti-neoplastic agents: current developments and promise of the PIH class of chelators. *Curr. Med. Chem.* 10, 1035-1049; (b) Campbell S. M., Morton C. A., Alyahya R., Horton S., Pye A., Curnow A. (2008). Clinical investigation of the novel iron - chelating agent, CP94, to enhance topical photodynamic therapy of nodular basal cell carcinoma. *Br. J. Dermatology* 159, 387-393; (c) Pye A., Campbell S., Curnow A. (2008). Enhancement of methyl-aminolevulinate photodynamic therapy by iron chelation with CP94: an in vitro investigation and clinical dose-escalating safety study for the treatment of nodular basal cell carcinoma. *J. Cancer Res. Clin. Oncology* 134, 841-849.
97. (a) Richardson D. R. (1997). Potential of iron chelators as effective antiproliferative agents. *Can. J. Physiol. Pharmacol.* 75, 1164-1180; (b) Rakba N., Loyer P., Gilot D., Delcros J. G., Glaise D., Baret P., Pierre J. L., Brissot P., Lescoat G. (2000). Antiproliferative and apoptotic effects of O-Trensox, a new synthetic iron chelator, on differentiated human hepatoma cell lines. *Carcinogenesis* 21, 943-951; (c) Bernhardt, P. V., Caldwell L. M., Chaston T. B., Chin P., Richardson D. R. (2003) Cytotoxic iron chelators: characterization of the structure, solution chemistry and redox activity of ligands and iron complexes of the di-2-pyridyl ketone isonicotinoyl hydrazone (HPKIH) analogues. *J. Biol. Inorg. Chem.* 8, 866-880; (d) Yuan J., Lovejoy D. B., Richardson D. R. (2004). Novel di-2-pyridyl-derived iron chelators with marked and selective antitumor activity: in vitro and in vivo assessment. *Blood* 104, 1450-1458; (e) Whitnall M., Howard J., Ponka P., Richardson D. R. (2006). A class of iron chelators with a wide spectrum of potent antitumor activity that overcome resistance to chemotherapeutics. *Proc. Natl. Acad. Sci. U.S.A.* 103, 14901-14906; (f) Fu D., Richardson D. R. (2007). Iron chelation and regulation of the cell cycle: Two mechanisms of post-transcriptional regulation of the universal cyclin-dependent kinase inhibitor p21CIP1/WAF1 by iron depletion. *Blood* 110, 752-761; (g) Kalinowski D. S., Richardson D. R. (2007) Future of Toxicology - Iron Chelators and Differing Modes of Action and Toxicity: The Changing Face of Iron Chelation Therapy. *Chem. Res. Toxicol.* 20, 715-720; (h) Simunek T., Sterba M., Popelova O., Kaiserova H., Adamcova M., Hroch M., Haskova P., Ponka P., Gersl V. (2008). Anthracycline toxicity to cardiomyocytes or cancer cells is differently affected by iron chelation with salicylaldehyde isonicotinoyl hydrazone. *Br. J. Pharm.* 155, 138-148; (i) Cappellini M. D., Pattoneri P. (2009). Oral iron chelators. *Ann. Rev. Med.* 60, 25-38; (j) Yu Y., Kalinowski D. S., Kovacevic Z., Siafakas A. R.,

- Jansson P. J., Stefani C., Lovejoy D. B., Sharpe P. C., Bernhardt P. V., Richardson D. R. (2009). Thiosemicarbazones from the Old to New: Iron Chelators That Are More Than Just Ribonucleotide Reductase Inhibitors. *J. Med. Chem.* 52, 5271-5294.
98. Horoszewicz JS, Kawinski E, Murphy GP, 1987, Monoclonal antibodies to a new antigenic marker in epithelial prostatic cells and serum of prostatic cancer patients, *Anticancer Res.*, **7**, 927-935.
99. Israeli RS, Powell CT, Fair WR, Heston WD, 1993, Molecular cloning of a complementary DNA encoding a prostate-specific membrane antigen, *Cancer Res.*, **53**, 227-230.
100. Schmittgen TD, Teske S, Vessella RL, True LD, Zakrajsek BA, 2003, Expression of prostate specific membrane antigen and three alternatively spliced variants of PSMA in prostate cancer patients, *Int. J. Cancer*, **107**, 323-329.
101. Carter RE, Feldman AR, Coyle JT, 1996, Prostate-specific membrane antigen is a hydrolase with substrate and pharmacologic characteristics of a neuropeptidase, *Proc. Natl. Acad. Sci. USA*, **93**: 749-753.
102. Silver DA, Pellicer I, Fair WR, Heston WD, Cordon-Cardo C, 1997, Prostate-specific membrane antigen expression in normal and malignant human tissues, *Clin. Cancer Res.*, **3**, 81-85.
103. Israeli RS, Powell CT, Corr JG, Fair WR, Heston WD, 1994, Expression of the prostate-specific membrane antigen, *Cancer Res.*, **54**, 1807-1811.
104. Babaian RJ, Sayer J, Podoloff DA, Steelhammer LC, Bhadkamkar VA, Gulfo JV, 1994, Radioimmunoscinigraphy of pelvic lymph nodes with ¹¹¹indium-labeled monoclonal antibody CYT-356, *J Urol.*, **152**, 1952-1955.
105. Kahn D, Williams RD, Manyak MJ, Haseman MK, Seldin DW, Libertino JA, Maguire RT, 1998, ¹¹¹Indium-capromab pendetide in the evaluation of patients with residual or recurrent prostate cancer after radical prostatectomy, *J. Urol.*, **159**, 2041-2047.
106. Kahn D, Williams RD, Seldin DW, Libertino JA, Hirschorn M, Dreicer M, Weiner GJ, Bushnell D, Gulfo J, 1994, Radioimmunoscinigraphy with ¹¹¹indium-labeled CYT-356 for the detection of occult prostate cancer recurrence, *J. Urol.*, **152**, 1490-1495.
107. Tjoa BA, Simmons SJ, Bowes VA, Ragde H, Rogers M, Elgamal A, Kenny GM, Cobb OE, Ireton RC, Troychak MJ, Salgaller ML, Boynton AL, Murphy GP, 1998, Evaluation of phase I/II clinical trials in prostate cancer with dendritic cells and PSMA peptides, *Prostate*, **36**, 39-44.
108. Murphy GP, Tjoa BA, Simmons SJ, Jarisch J, Bowes VA, Ragde H, Rogers M, ElgamalA, KennyGM, Cobb OE, Ireton RC, Troychak MJ, Salgaller ML, Boynton AL, 1999, Infusion of dendritic cells pulsed with HLA-A2-specific prostate-specific membrane antigen peptides: A phase II prostate cancer vaccine trial involving patients with hormone-refractory metastatic disease, *Prostate*, **38**, 73-78.
109. Huang X, Bennett M, Thorpe PE, 2004, Anti-tumor effects and lack of side effects in mice of an immunotoxin directed against human and mouse prostate-specific membrane antigen, *Prostate*, **61**, 1-11.
110. Mhaka A, Gady AM, Rosen DM, Lo KM, Gillies SD, Denmeade SR, 2004, Use of Methotrexate-Based Peptide Substrates to Characterize the Substrate Specificity of Prostate-Specific Membrane Antigen (PSMA), *Cancer Biol. Ther.*, **3**, 551-558.
111. Louie AY, Meade TJ, 2000, Recent advances in MRI: Novel contrast agents shed light on *in-vivo* biochemistry, *TiBS*, 7-11.

Prostate Cancer Evaluation: Design, Synthesis and Evaluation of Novel Enzyme-Activated ¹H MRI Contrast Agents

112. Jackson PF, Slusher BS, 2001, Design of NAALADase: A novel neuroprotective strategy, *Curr. Med. Chem.*, **8**, 949-957.
113. O'Keefe DS, Su SL, Bacich DJ, 1998, Mapping, genomic organization and promoter analysis of the human prostate-specific membrane antigen gene, *Biochim. Biophys. Acta*, **1443**, 113-127.

APPENDICES

- (1) Jian-Xin Yu, R. P. Mason, Design and Synthesis of Novel *lacZ* Responsive Enhanced MRI Agent, *The World Molecular Imaging Conference*, #0614, Montreal, Canada, September 23-26, 2009.
- (2) Jian-Xin Yu, Dawen Zhao, R. P. Mason, Design and Synthesis of Novel *lacZ* Responsive Enhanced MRI Agent, *The World Molecular Imaging Conference*, #0615, Montreal, Canada, September 23-26, 2009.

DEVELOPMENT OF NOVEL Fe-BASED ¹H MRI *lacZ* GENE REPORTERS FOR *IN VIVO* ASSESSMENT

**SOUTHWESTERN
MEDICAL CENTER**

Jian-Xin Yu, Dawen Zhao, Ralph P. Mason

Cancer Imaging Program, Department of Radiology

Presentation: 0614

University of Texas Southwestern Medical Center at Dallas, Texas, USA



INTRODUCTION

The *lacZ* gene encoding β-galactosidase (β-gal) has been recognized as the most attractive reporter gene, and its introduction has become a standard means of assaying clonal insertion, transcriptional activation, protein expression, and protein interaction. Therefore, its noninvasive *in vivo* detection would be of considerable value in many ongoing and future clinical cancer gene therapy trials.^[1] To this end, a variety of *in vivo lacZ* gene reporters has been developed, such as colorimetric,^[2] fluorescent,^[3-5] bioluminescent,^[6] radiotracers for positron emission tomography (PET) or single-photon emission computed tomography (SPECT),^[7,8] magnetic resonance imaging (MRI) probes^[9,11] and ²³F magnetic resonance spectroscopy (MRS) and chemical shift imaging (CSI) reporters.^[12-14] We now report the development of a new class of Fe-based ¹H MRI *lacZ* gene reporters based on clinically applied iron-depletion agents.

Iron is a critically important metal ion for a wide variety of cellular events. Tumor cells, as compared with their normal counterparts, frequently exhibit increased uptake and utilization of more iron. Many studies indicate that a high level of iron accumulated in animals and humans is associated with both the initiation and the progression of cancers. Cancer cells are also sensitive to iron depletion because of the critical requirement for iron in proteins that play essential roles in DNA synthesis, repair and energy production. Iron depletion as a therapeutic strategy has been applied for cancers. The FDA has already approved five iron chelators for use in anticancer therapy, others are being evaluated in clinical settings.^[15]

Based on the structural similarities between the iron complexes with the clinically applied iron depletion agents and the known Fe-based ¹H MRI contrast agents, we firstly demonstrated that the clinically applied Fe-chelators can act as Fe-based ¹H MRI contrast agents producing strong contrast effects (Table 1), opening a new era of iron depletion agent as anticancer drug as well as of ¹H MRI detection or diagnosis agent.

Chelator	SBH	SIH	SNH
T ₁ -weighted ¹ H MRI (Control)			
T ₁ -weighted ¹ H MRI (Complex)			

Table 1. ¹H-MRI Function of the Fe-Complexes with the clinically applied iron depletion agents: salicylaldehyde benzoyl hydrazine (SBH), salicylaldehyde isonicotinoyl hydrazine (SIH) and its analog salicylaldehyde nicotinoyl hydrazine (SNH). [Conditions: T₁-weighted ¹H MRI, 200MHz, TR=300ms, TE=20ms, 1.5mm slice, 128-128, 50-50mm². (A) Control, FAC (2.5μmol), PBS (1.5mL); (B) Complex, SBH, SIH or SNH each (5μmol), FAC (2.5μmol), PBS (1.5mL).]

MOLECULAR DESIGN

Prompted by this finding, we now propose a novel molecular design to deliver the *in situ* formation of Fe-complexes of iron depletion agents specific targeting on cancer by using Gene Directed Enzyme Prodrug Therapy (GDEPT) strategy.

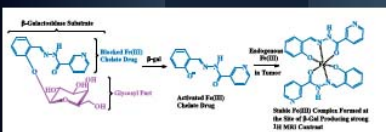


Figure 1. The proposed new ¹H MRI approach for *in vivo* detection of *lacZ* gene expression through the *in situ* formation of Fe-complexes of iron depletion agents.

MOLECULAR DESIGN

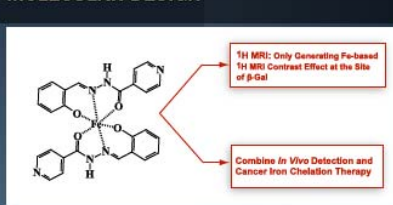


Figure 2. The proposed new ¹H MRI approach for *in vivo* detection of *lacZ* gene expression through the *in situ* formation of Fe-complexes of iron depletion agents, combining *in vivo* detection and cancer iron chelation therapy.

TARGET MOLECULE SYNTHESIS

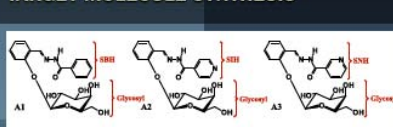
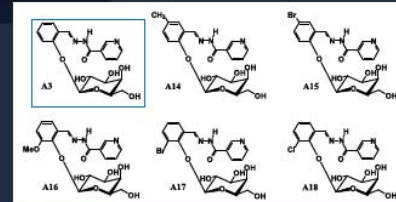
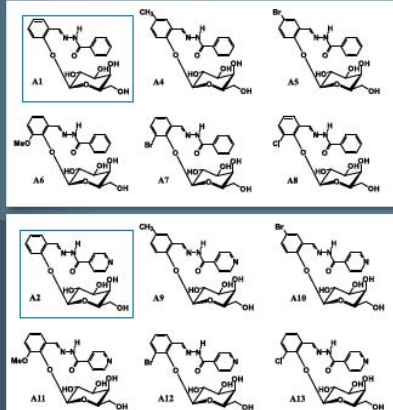


Figure 3. The Structures of the Target Molecules

ALTERNATE MOLECULE SYNTHESIS

Considering the multiple requirements for an ideal *in vivo* reporter, we designed a series of alternate candidates based on the different substituents at different positions, which shall be directly related to the enzyme sensitivity and specificity, aqueous solubility, toxicity, and importantly, the ability of the released arylhydrazones to complex Fe²⁺ ion (Fe-based ¹H MRI effects).



RESULTS

Testing A1-A18 with β-galactosidase G-5160, showed that all, except A7, A8, A12 and A13, can react with β-galactosidase G-5160 in the presence of Fe²⁺. The released iron depletion agents then spontaneously capture Fe²⁺ readily *in situ* forming stable Fe-complexes, which produce strong Fe-based ¹H MRI contrast.

Reporters	A1	A2	A3	A4	A5	A6	A9
T ₁ -weighted ¹ H MRI (Control)							
T ₁ -weighted ¹ H MRI (Complex)							

Reporters	A10	A11	A14	A15	A16	A17	A18
T ₁ -weighted ¹ H MRI (Control)							
T ₁ -weighted ¹ H MRI (Complex)							

Table 2. ¹H-MRI contrast of the reporters A1-A6, A9-A11 and A14-A18 in the presence of FAC. [Conditions: T₁-weighted ¹H MRI, 200MHz, TR=300ms, TE=20ms, 1.5mm slice, 128-128, 50-50mm². (A) Control, A1-A6, A9-A11 and A14-A18 each (5μmol), FAC (2.5μmol), PBS (0.1M, pH=4.5, 1.5mL); (B) Complex, A1-A6, A9-A11 and A14-A18 each (5μmol), FAC (2.5μmol), G-5160 (5 units), PBS (0.1M, pH=4.5, 1.5mL).]

CONCLUSIONS

These molecules demonstrate the feasibility of combining anticancer drug iron depletion agents for detection of the *lacZ* reporter gene, opening a new possibility of merging cancer therapy and detection into one approach.

REFERENCES

1. Ghadiri A, *NMR Biomed.*, 2007, 20, 275.
2. Li L, *J. Biomed. Opt.*, 2007, 12, 020504.
3. Tang QH, *et al.*, *Cancer Res.*, 2004, 64, 1578.
4. Ueno Y, *et al.*, *J. Am. Chem. Soc.*, 2005, 127, 4088.
5. Kamaya M, *et al.*, *J. Am. Chem. Soc.*, 2007, 129, 7045.
6. Weisman TS, *et al.*, *Nat. Methods.*, 2006, 3, 295.
7. Lee KH, *et al.*, *Eur. J. Nucl. Med. Mol. Imaging.*, 2004, 31, 433.
8. Cohen S, *et al.*, *Bioconjugate Chem.*, 2009, 19, 441.
9. Van Dam ME, *et al.*, *Mol. Imaging.*, 2006, 7, 187.
10. Lewis AJ, *et al.*, *Angew. Chem. Int. Ed. Engl.*, 1999, 38, 726.
11. Chang Y, *et al.*, *Bioconjugate Chem.*, 2007, 18, 1716.
12. Liu L, *et al.*, *FASEB J.*, 2007, 21, 2014.
13. Yu JX, *et al.*, *Magn. Reson. Med.*, 2008, 21, 704.
14. Kodhagur VD, *et al.*, *Magn. Reson. Imaging.*, 2006, 24, 99.
15. Capellan MD, *et al.*, *Ann. Rev. Med.*, 2009, 60, 23.

ACKNOWLEDGEMENT

This work is supported in part by DOD Prostate Cancer New Investigator Award W81XWH-05-1-0593 (JXY) and NCI R21 CA04095 (RPM). Investigations are facilitated by the Southern Texas Small Animal Imaging Research Program, funded in part by NCI U24 CA126408 and NMR experiments are conducted at the Mary Nell and Ralph B. Rogers NMR Facility at NIH ETRP facility P41-RR02584, and component of the AIBC.



DEVELOPMENT OF NOVEL *lacZ* RESPONSIVE ENHANCED Gd-BASED MRI AGENT

Jian-Xin Yu, Ralph P. Mason

Cancer Imaging Program, Department of Radiology

University of Texas Southwestern Medical Center at Dallas, Texas, USA

SOUTHWESTERN
MEDICAL CENTER

Presentation: 0615



INTRODUCTION

Gene therapy holds great promise for treating cancer and has been successfully exploited in several clinical trials. A major current obstacle to implementation is to establish a method of assessment of therapeutic gene expression in terms of heterogeneity and longevity in tissues. The *lacZ* gene encoding β -galactosidase (β -gal) has been recognized as the most attractive reporter gene. Therefore, noninvasive detection *in vivo* would be of considerable value in future clinical cancer gene therapy trials.^[1] Various groups have presented innovative approaches to assessing β -gal activity *in vivo* using gadolinium enhanced contrast ¹H MRI or ¹⁹F NMR spectroscopy,^[2-4] optical^[5-10] and radionuclide imaging.^[11-16] We now report the exploration of a novel approach to *lacZ* responsive Gd-based ¹H MRI agents.

Desreux *et al.* demonstrated that, by chelating Gd(phen)HDO₃A with Fe(II) to form a highly stable tris-complex, the relaxivity increased 145% at 20 MHz and 37°C.^[17] Most recently, Tóth *et al.* showed that the heterometallic, self-assembled metallostar with six efficiently relaxing Gd(III) centers, [Fe(Gd₄L(H₂O))₆]⁴⁺, exhibited a particularly high relaxivity for its moderate molecular weight.^[18]

Iron is a critically important metal ion for a wide variety of cellular events. Tumor cells, as compared with their normal counterparts, frequently exhibit increased uptake and utilization of more iron. Many studies indicate that a high level of iron accumulation in animals and humans is associated with both the initiation and the progression of cancers. Cancer cells are also sensitive to iron depletion because of the critical requirement for iron in proteins that play essential roles in DNA synthesis, repair and energy production. Iron depletion as a therapeutic strategy has been applied for cancers. The FDA has already approved five iron chelators for use in anticancer therapy; others are being evaluated in clinical settings.^[19]

DESIGN

Prompted by this finding, we now propose a novel class of enzyme activated Gd³⁺-based MRI contrast agent for *in vivo* detection of β -gal activity combining three features: (A) a signal enhancement group, such as Gd-DTTA; (B) an Fe³⁺ chelating group using the structure of clinical iron chelation therapy drugs; (C) β -D-galactose. Following cleavage by β -gal in cells, the released, activated glycone Fe³⁺-ligand will spontaneously trap endogenous Fe³⁺ at the site of enzyme activity forming a highly stable complex, exhibiting restricted motion of the Gd³⁺ chelates enhancing relaxivity and providing contrast based on gene (*viz.* enzyme) stimulated local accumulation (Figure 1).

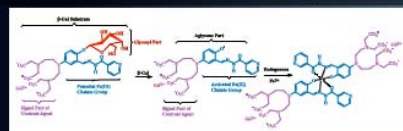
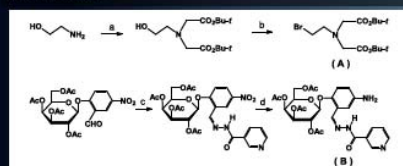


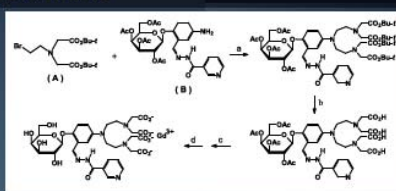
Figure 1. The proposed new mechanism for *in vivo* detection of *lacZ* gene expression through Fe³⁺-trapped MRI contrast agent formation.

SYNTHESIS



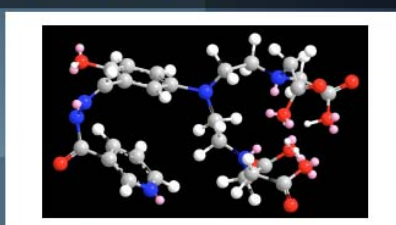
Reaction Conditions: (a) BrCH₂CO₂Bu-t, K₂CO₃, 88%; (b) Ph₃P, NBS, 86%; (c) Nicotinic Hydrazide, EtOH, AcOH, Reflux, 85%; (d) H₂, Pd/C, 94%.

SYNTHESIS

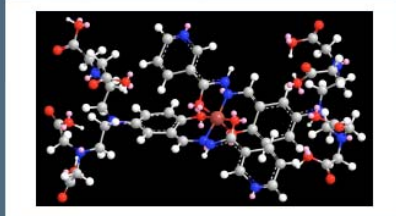


Reaction Conditions: (a) K₂CO₃, MeCN, 38%; (b) CF₃CO₂H, CH₂Cl₂, 52%; (c) GdCl₃, Pyridine, 57%; (d) MeOH, MeONa, 75%.

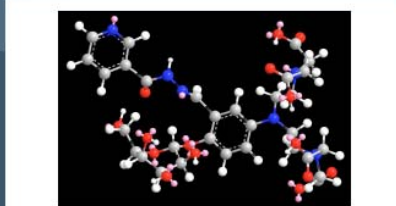
STRUCTURAL FEATURES



Ligand Structure

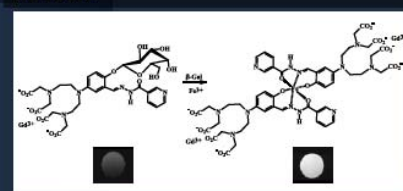


Fe-Complex Structure



Conjugate Structure

RESULTS



Conditions: T₂-weighted 2H MRI, 200MHz, TR=300ms, TE=20ms, 1.5mm slice, 128x128, 50-50mm². (A) Control, sample (5μmol), FAC (2.5μmol), PBS (0.1M, pH=4.5, 1.5mL); (B) Complex, sample (5μmol), FAC (2.5μmol), G-5160 (5 units), PBS (0.1M, pH=4.5, 1.5mL).

CONCLUSIONS

We propose a novel class of enzyme activated Gd³⁺-based MRI contrast agent for detection of β -gal activity. Synthesis of the substrate has been successful, and the evaluation of this agent with β -gal showed that the released glycone including the activated Fe³⁺-ligand and MRI signal enhancement group spontaneously traps Fe³⁺ in the solution forming a highly stable complex, then restricting the motion of the Gd³⁺ chelates enhancing relaxivity. We are now evaluating this agent with β -gal expressing cells and *in vivo*.

REFERENCES

- Gilad *et al.*, NMR Biomed., 2007, 20, 275.
- Lodde AV *et al.*, Nature Biotechnology, 2000, 18, 321.
- Chang Y T *et al.*, Bioconjugate Chem., 2007, 18, 1716.
- Liu L *et al.*, FASEB J., 2007, 21, 2014.
- Yi J X *et al.*, Magn. Reson. Med., 2008, 21, 704.
- Kodhugkar VD *et al.*, Magn. Reson. Imaging, 2006, 24, 959.
- Li L *et al.*, J. Biomed. Opt., 2007, 12, 020504.
- Ting CH *et al.*, Cancer Res., 2004, 64, 1579.
- Umano Y *et al.*, J. Am. Chem. Soc., 2005, 127, 4888.
- Kamiya M *et al.*, J. Am. Chem. Soc., 2007, 129, 3918.
- Wehrman TS *et al.*, Nat. Methods, 2006, 3, 295.
- Lee KH *et al.*, Eur. J. Nucl. Med. Mol. Imaging, 2004, 31, 433.
- Celes S *et al.*, Bioconjugate Chem., 2008, 19, 441.
- Van Dort ME *et al.*, Mol. Imaging, 2008, 7, 152.
- Desreux *et al.*, (a) Topics Curr. Chem., 2002, 221, 123; (b) Chemistry of Contrast Agents in Medical Magnetic Resonance Imaging, 2004, 157.
- Mehlich *et al.*, Chem. Rev., 2005, 105, 1925.
- Cappelloni MD *et al.*, Ann. Rev. Med., 2009, 60, 25.

ACKNOWLEDGEMENT

This work is supported by DOD Prostate Cancer New Investigator Award W81XWH-05-1-0593 (JXY). Investigations are facilitated by the Southwestern Small Animal Imaging Research Program, funded in part by NCI U24 CA126608 and NMR experiments are conducted at the Mary Nell and Ralph B. Rogers NMR Facility an NIH BTRP facility P41-RR02594, and component of the AIRC.

ADDITIONAL INFORMATION

For additional information, please contact:

Jian-Xin Yu@UTSouthwestern.edu

